Balancing exposed and hidden nodes in linear wireless networks

P.M. van de Ven, A.J.E.M. Janssen, *Fellow, IEEE* and J.S.H. van Leeuwaarden

***Abstract*—Wireless networks equipped with the CSMA protocol are subject to collisions due to interference. For a given interference range we investigate the tradeoff between collisions (hidden nodes) and unused capacity (exposed nodes). We show that the sensing range that maximizes throughput critically depends on the activation rate of nodes. For infinite line networks, we prove the existence of a threshold: When the activation rate is below this threshold the optimal sensing range is small (to maximize spatial reuse). When the activation rate is above the threshold the optimal sensing range is just large enough to preclude all collisions. Simulations suggest that this threshold policy extends to more complex linear and non-linear topologies.**

***Index Terms*—Carrier-sensing range, collisions, exposed nodes, hidden nodes, Markov processes, random-access, throughput, wireless networks**

I. Introduction

Carrier sense multiple-access (CSMA) type protocols form a popular class of medium access protocols for wireless networks. The first CSMA protocol was introduced by Kleinrock and Tobagi [16] in 1975, and has seen many incarnations since, including the widely used 802.11 standard. In this paper we provide an asymptotic analysis of large wireless networks operating under CSMA, in the presence of collisions.

CSMA is a randomized protocol that allows nodes to access the medium in a distributed manner. The absence of a centralized scheduler creates more flexibility and allows for the deployment of larger networks. An early example of such a randomized procedure is the ALOHA protocol [1], which forces nodes to wait for some random backoff period before starting a transmission, in order to reduce the likelihood of nearby nodes transmitting simultaneously. The latter event would cause the signals to interfere with each other, and may result in a collision that renders the transmissions useless. CSMA improves upon ALOHA by letting nodes *sense* their surroundings to detect the presence of other transmitting nodes. If a node detects at least one active (i.e. transmitting) node within its sensing range, its backoff timer is frozen, deferring the countdown until the channel is sensed clear. Using this mechanism, collisions can be further reduced.

A key performance measure in wireless networks is throughput, which we define as the average number of successful transmissions per unit of time. We investigate the relation between the sensing range and the throughput. The effect of the sensing range can be understood as follows. A small sensing range allows for more simultaneous transmissions, but is less effective in reducing collisions. On the other hand, a large sensing range admits fewer transmissions, but also mitigates interference. The main contribution of this paper is the examination of this tradeoff in relation to its effect on the throughput.

The network is characterized by the sensing range and the interference range. A node can only initiate a new transmission when all nodes within its sensing range are inactive. This transmission is successful when all nodes within the interference range of the destination node are inactive, and fails otherwise. The network performance suffers from two complementary issues: hidden nodes and exposed nodes (see [16]). Hidden nodes are nodes located outside the sensing range of the transmitter and are therefore not detected by the carrier-sensing mechanism. Hidden nodes cause collisions as they are within the receiver's interference range. Exposed nodes are nodes located outside the receiver's interference range but inside the sender's sensing range. So despite being harmless to the transmission, exposed nodes are nevertheless blocked. As the sensing range grows, the number of hidden nodes decreases, and the number of exposed nodes increases.

In recent years the performance issues caused by hidden and exposed nodes have been extensively studied in research literature. Various studies look modifying the CSMA algorithm to eliminate either hidden or exposed nodes, for example by using separate control channels [20], through busy tone signals [12], [19] or by modifying and temporarily disabling the carrier-sensing mechanism [13]. However, no such approach is successful in simultaneously eliminating hidden and exposed nodes, and solving either issue may exacerbate the other. In general, eliminating both hidden and exposed nodes is considered to be a very difficult problem [13].

Thus, rather than modifying the CSMA algorithm, we want to balance hidden and exposed nodes by carefully choosing the sensing range. The problem of finding the sensing range that maximizes throughput has received considerable attention in recent years [11], [17], [18], [27], [29], [30]. Although these works each consider a distinct physical-layer and MAC-layer model, all treat exposed and hidden nodes in a similar manner. That is, they assume for each transmission the existence of a hidden (exposed) node area such that this transmission will collide (be blocked) if any node in this area is active. Rather than analyzing a fixed network structure, hidden and exposed node events are then approximated by assuming a randomized topology and computing the probability of an active hidden

A preliminary version of this paper appeared as [24]

P.M. van de Ven is with the IBM Thomas J. Watson Research Center, Yorktown Heights, NY 10598, USA (e-mail: pmvandev@us.ibm.com)

A.J.E.M. Janssen is with Eurandom and the Eindhoven University of Technology, Department of Electrical Engineering, 5600 MB Eindhoven, The Netherlands (e-mail: a.j.e.m.janssen@tue.nl)

J.S.H. van Leeuwaarden is with the Eindhoven University of Technology, Department of Mathematics and Computer Science, 5600 MB Eindhoven, The Netherlands (e-mail: j.s.h.v.leeuwaarden@tue.nl)

or exposed node by multiplying the size of these areas by the node density, and assuming that nodes operate independently from each other.

This approach ignores both the network structure and complex interactions between nodes in a random-access network, and provides only a crude approximation of the carrier-sensing tradeoff. In the present paper we consider a fixed network topology, and propose a model that does take into account the node interactions, by keeping track of the activity of the nodes over time. Careful analysis of the resulting Markov chain model allows us to demonstrate that the optimal sensing range in fact depends on the activation rate of the nodes.

The classical model for such interaction in wireless networks is developed in Boorstyn and Kershenbaum [5]. This model is a special instance of a loss network [15], and has been used in recent years to study throughput-optimality [4], [14], [21], [23] and fairness [8], [9], [25], [26] in a setting without collisions. The stability region for large wireless networks with collisions was investigated in [6].

In the spirit of [5], we model the network as a continuous-time Markov process with interaction between the nodes, so that nodes within a certain distance of an active node are silenced, just as in CSMA. Such interaction is referred to in statistical physics as *hard-core* interaction. Typical for such models is the existence of a Gibbs measure that describes the stationary distribution. This Gibbs measure is normalized by the partition function, which involves a computationally cumbersome summation over all possible configurations. A substantial ingredient of this paper is to characterize and approximate the partition function. We shall consider the network, and thus the partition function, in the asymptotic regime where the number of nodes in the network tends to infinity. For such infinite line networks we are able to obtain structural results on the joint effect of hidden nodes and exposed nodes.We determine analytically the throughput-optimal sensing range that achieves the best tradeoff between reducing hidden nodes and preventing exposed nodes.

We propose a novel model for evaluating the effect of exposed and hidden nodes on throughput. In contrast to existing such models we keep track of node activity over time, and capture the effect of higher-order node interactions on network performance. This model reveals various surprising results that cannot be derived in the existing simplified models; our main findings are as follows:

- The throughput-optimal sensing range β^* depends on the activation rate σ. The β^* takes values in some bounded interval, and increases with σ;
- For regular networks, the transition from β^* small to β^* large is very sudden;
- The network topology and transmission distance have a significant impact on β^*.

The remainder of this paper is structured as follows. In Section II we introduce the model, and derive some auxiliary results. Section III discusses the main results on the carrier-sensing tradeoff. In Section IV we perform a detailed study of the partition function. In Section V we validate the analytical results for the line network by simulation, and we investigate networks with more general topologies. In Section VI we present the proofs of those results that are not already proved in earlier sections.

II. Model description

We consider a linear array of $2n+1$ nodes, and we denote the set of all nodes by $\mathcal{N} = \{-n, \dots, n\}$. We fix the transmission distance Δ, and assume that whenever a node activates, it transmits a single packet to either the node Δ hops to its right (with probability ψ) or to the node Δ hops to its left (with probability $1-\psi$). To accommodate this, we introduce (pure destination) nodes $n+1, \dots, n+\Delta$ and $-(n+1), \dots, -(n+\Delta)$, which receive packets, but do not transmit packets themselves. The case $\Delta = 1$ corresponds to nearest-neighbor transmissions, where nodes can only transmit packets over a single hop. For $\Delta \geq 2$, nodes are allowed to skip their immediate neighbors. As will be shown in Proposition 2, the throughput is insensitive to the parameter ψ. We assume that all nodes are saturated, meaning that they have an infinite supply of packets available for transmission.

After each transmission nodes enter a backoff period, meaning that they will remain inactive for some time. The length of the backoff period is assumed to be exponentially distributed with mean $1/\sigma$. We assume all nodes to have the same sensing range β, so that node v is prohibited from transmitting whenever at least one node w for which $|v-w| \leq \beta$ is active (i.e. transmitting), in which case we say that node v is *blocked* by node w. So when a node finishes its backoff period and it finds at least one node within distance β active, it enters a new backoff period. When a node finds all nodes within distance β inactive upon finishing backoff, it starts a transmission. Transmissions last for an exponentially distributed duration with unit mean. Under these assumptions, the $(2n+1)$-dimensional process that describes the activity of nodes is a continuous-time Markov process. Each state of the Markov process is described by

$$\omega = (\omega_{-n}, \dots, \omega_n) \in \{0,1\}^{2n+1}, \tag{1}$$

where $\omega_v = 1$ when node v is active, and $\omega_v = 0$ otherwise. Let $\Omega \subseteq \{0,1\}^{2n+1}$ be the set of all *feasible* states. Here we call ω feasible if no two 1's in ω are β positions or less apart, i.e., $\omega_v \omega_w = 0$ if $1 \leq |v-w| \leq \beta$. Let e_v denote the vector with all zeros, except for a 1 at position v. The Markov process that describes the activity of nodes is then fully specified by the state space Ω and the transition rates

$$r(\omega, \omega') = \begin{cases} \sigma & \text{if } \omega' = \omega + e_v, \\ 1 & \text{if } \omega' = \omega - e_v, \\ 0 & \text{otherwise.} \end{cases} \tag{2}$$

It is well known that this is a reversible Markov process (see [5], [22]) with limiting distribution

$$\pi(\omega) = \begin{cases} Z_{2n+1}^{-1} \prod_{v=-n}^{n} \sigma^{\omega_v} & \text{if } \omega \text{ is feasible,} \\ 0 & \text{otherwise,} \end{cases} \tag{3}$$

with Z_{2n+1} the partition function or normalization constant of the probability distribution π. The partition function can be defined recursively as (see [5], [22])

$$Z_i = \begin{cases} 1 + i\sigma & i = 0, 1, \dots, \beta+1, \\ Z_{i-1} + \sigma Z_{i-\beta-1} & i \geq \beta+2. \end{cases} \tag{4}$$

The sequence $(Z_i)_{i=0}^{\infty}$ is well studied. In fact, for a network with i nodes, Z_i represents the partition function, defined as the summation of probability over all possible states. Straightforward calculations show that the the generating function $G_Z(x)$ of Z_i can be written as (see e.g. Pinksy and Yemini [22])

$$G_Z(x) = \sum_{i=0}^{\infty} Z_i x^i = \frac{x - 1 + \sigma x^{\beta+1} - \sigma x}{(x-1)(1 - x - \sigma x^{\beta+1})}. \quad (5)$$

Let $\lambda_0, \ldots, \lambda_\beta$ denote the $\beta + 1$ distinct roots (see Proposition 8) of

$$\lambda^{\beta+1} - \lambda^{\beta} - \sigma = 0. \quad (6)$$

We denote by λ_0 the unique positive real root for which $\lambda_0 > |\lambda_j|,\ j \neq 0$ (see [22]). Applying partial fraction expansion to (5) yields the following result (proved in Section VI):

Proposition 1. *The partition function Z_i is given by*

$$Z_i = \sum_{j=0}^{\beta} c_j \lambda_j^i \quad , i = 0, 1, \ldots, \quad (7)$$

where λ_j are the roots of (6)*, and*

$$c_j = \frac{\lambda_j^{\beta+1}}{(\beta+1)\lambda_j - \beta}. \quad (8)$$

The proof of Proposition 1 is provided in Appendix VI, along with the other proofs not given in the main text.

To model interference, we introduce an interference range $\eta \geq \Delta$. A transmission succeeds if and only if at the start of this transmission no nodes within distance η of the receiving node are already active. This type of interference is referred to in the literature as the *perfect capture* collision model [5]. Note that neither (2) nor (3) depends on η, as collisions have no impact on the dynamics of the system. Using the sensing range β and interference range η we can define formally hidden nodes and exposed nodes. Consider a transmission from node v to node w. Hidden nodes are then defined as nodes that are outside the sensing range of v, but within the interference range of w. Such nodes are not blocked by the activity of node v, but their proximity to node w makes the hidden nodes harmful to the transmission from v to w. Conversely, exposed nodes are those nodes that are within the sensing range of v, but outside the interference range of w. Such nodes are blocked by an ongoing transmission from v to w, despite the fact that they will not cause this transmission to fail. Denote by $\mathcal{H}_r$ ($\mathcal{H}_l$) the set of hidden nodes of transmissions from node 0 to node Δ (node -Δ): all nodes outside the sensing range of 0, but within the interference range of the receiving node Δ (node -Δ). By $\mathcal{E}_r$ ($\mathcal{E}_l$) we denote the set of nodes to which this transmission is exposed, so all nodes within the sensing range of 0, but outside the interference range of the receiving node. For completeness we let $\mathcal{B}_r$ ($\mathcal{B}_l$) denote the set of all remaining nodes that block transmissions from node 0 to node Δ (node -Δ). This yields:

$$\begin{aligned}
\mathcal{H}_r &= \{ v \in \mathcal{N} \mid |v| \geq \beta + 1,\ |v - \Delta| \leq \eta \}, \\
\mathcal{H}_l &= \{ v \in \mathcal{N} \mid |v| \geq \beta + 1,\ |v + \Delta| \leq \eta \}, \\
\mathcal{E}_r &= \{ v \in \mathcal{N} \mid |v| \leq \beta,\ |v - \Delta| \geq \eta + 1 \}, \\
\mathcal{E}_l &= \{ v \in \mathcal{N} \mid |v| \leq \beta,\ |v + \Delta| \geq \eta + 1 \}, \\
\mathcal{B}_r &= \{ v \in \mathcal{N} \mid |v| \leq \beta,\ |v - \Delta| \leq \eta \}, \\
\mathcal{B}_l &= \{ v \in \mathcal{N} \mid |v| \leq \beta,\ |v + \Delta| \leq \eta \}.
\end{aligned}$$

So $\mathcal{E}_r \cup \mathcal{B}_r = \mathcal{E}_l \cup \mathcal{B}_l = \{ v \in \mathcal{N} \mid |v| \leq \beta \}$. An example with $\Delta = 1$ is given in Figure 1(a). Node 3 is a hidden node, as it interferes with the transmission from node 0 to node 1 ($\eta = 2$) despite the carrier-sensing mechanism ($\beta = 1$). In Figure 1(b) node 0 is an exposed node to the transmission from node 2 to node 3 because it would not interfere ($\eta = 2$) with this transmission but is nevertheless silenced by the activity of node 2 ($\beta = 2$).

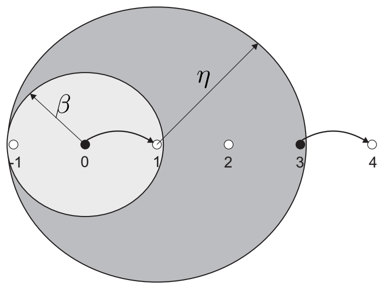

(a) Node 3 is a hidden node, and may interfere with the transmission between nodes 0 and 1.

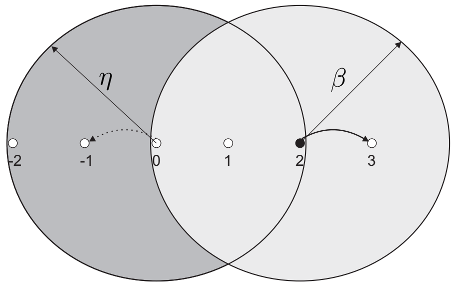

(b) Node 0 is an exposed node, unnecessarily silenced by the transmission between nodes 2 and 3.

Fig. 1. Examples of hidden and exposed nodes.

We focus on node 0 (the node in the middle of the network) and in particular its throughput $\theta_n(\beta, \eta, \sigma)$ defined as the average number of successful transmissions per unit of time.

Proposition 2. *The throughput of node 0 is given by*

$$\theta_n(\beta, \eta, \sigma) = \sigma \frac{Z_{n - \max\{\beta, \eta - \Delta\}} Z_{n - \max\{\beta, \eta + \Delta\}}}{Z_{2n+1}}. \quad (9)$$

Proof: Denote by θ_r (θ_l) the rate of successful transmission of node 0 to node Δ (node -Δ), so $\theta_n(\beta, \eta, \sigma) = \theta_r + \theta_l$. The activation attempts to node Δ (node -Δ) occur according to a Poisson process with rate $\sigma\psi$ (rate $\sigma(1 - \psi)$). We first consider activation attempts towards node Δ . Whether an activation attempt is successful depends on the state of the system when this attempt occurs. Define

$$A_1 = \{\, \omega \in \Omega \mid \exists v \in \mathcal{B}_r \cup \mathcal{E}_r : \omega_v = 1 \,\},$$
$$A_2 = \{\, \omega \in \Omega \mid \forall v \in \mathcal{B}_r \cup \mathcal{E}_r : \omega_v = 0,\ \exists v \in \mathcal{H}_r : \omega_v = 1 \,\},$$
$$A_3 = \{\, \omega \in \Omega \mid \forall v \in \mathcal{B}_r \cup \mathcal{E}_r \cup \mathcal{H}_r : \omega_v = 0 \,\}.$$

When the system is in state $\omega \in A_1$, the attempt is blocked and node 0 remains in its current state. When the system is in a state $\omega \in A_2$, node 0 is not blocked so it activates. However, at least one hidden node is active so the transmission fails and does not contribute to the throughput. When the system is in state $\omega \in A_3$, the perfect capture assumption guarantees a successful transmission. It follows from the PASTA property (cf. [2]) that the probability of an arbitrary activation attempt resulting in a successful transmission is equal to the limiting probability of the system being in a state $\omega \in A_3$. So the rate of successful transmissions initialized (and thus the throughput) is given by

$$\theta_r = \sigma\psi \sum_{\omega \in A_3} \pi(\omega). \tag{10}$$

From the definitions of $\mathcal{B}_r$, $\mathcal{E}_r$ and $\mathcal{H}_r$ we see that

$$A_3 = \{\, \omega \in \Omega \mid \forall v \in (D_1 \cup D_2)^c : \omega_v = 0 \,\}, \tag{11}$$

where

$$D_1 = \{-n, \dots, -\max\{\beta, \eta - \Delta\} - 1\},$$
$$D_2 = \{\max\{\beta, \eta + \Delta\} + 1, \dots, n\}. \tag{12}$$

Let Z_D denote the partition function for a subset of nodes $D \subseteq \mathcal{N}$ defined as $Z_D = \sum_{\omega \in \Omega,\ \forall v \in D^c : \omega_v = 0} \prod_{v=-n}^{n} \sigma^{\omega_v}$. Then

$$\theta_r = \sigma\psi \frac{Z_{D_1 \cup D_2}}{Z_{\mathcal{N}}}. \tag{13}$$

The model on the line has the property that by conditioning on the activity of one of the nodes, its state space can be decomposed, leading to two smaller instances of the same model on the line. In particular, we know that $Z_{D_1 \cup D_2} = Z_{D_1} Z_{D_2}$ (see [5, Equation (15)]), so that

$$\begin{aligned} \theta_r &= \sigma\psi \frac{Z_{D_1} Z_{D_2}}{Z_{\mathcal{N}}} \\ &= \sigma\psi \frac{Z_{n-\max\{\beta,\eta-\Delta\}} Z_{n-\max\{\beta,\eta+\Delta\}}}{Z_{2n+1}}, \end{aligned} \tag{14}$$

where Z_i denotes the partition function of a network with i consecutive nodes on a line. Similarly,

$$\theta_l = \sigma(1-\psi) \frac{Z_{n-\max\{\beta,\eta-\Delta\}} Z_{n-\max\{\beta,\eta+\Delta\}}}{Z_{2n+1}}. \tag{15}$$

and (9) follows by adding θ_r and θ_l. ■

III. Main results

Our principal aim is to choose the sensing range β so that the throughput $\theta_n(\beta, \eta, \sigma)$ is maximized for a given η and σ. Define

$$\beta_n^* = \operatorname*{argmax}_{\beta} \theta_n(\beta, \eta, \sigma). \tag{16}$$

Determining β_n^* corresponds to quantifying and optimizing the tradeoff between preventing collisions through interference (preventing hidden nodes by setting β large) and allowing harmless transmissions (preventing exposed nodes by setting β small). We want to obtain structural insights in how to choose β_n^*, and for this purpose the expressions for Z_i in (7) and $\theta_n(\beta, \eta, \sigma)$ in (9) are too cumbersome. Therefore, we investigate the throughput in the regime where the network becomes large ($n \to \infty$), so that (9) simplifies considerably, allowing for more explicit analysis. The analytic results that we obtain for the infinite network provide remarkably sharp approximations for the finite network; see Section III-B. All proofs that are not given in this section are provided in Section VI.

We start by presenting the limiting expression for $\theta_n(\beta, \eta, \sigma)$ as the size of the network becomes infinite:

Proposition 3. *Let λ_0 denote the unique positive real root of* (6)*. Then*

$$\theta(\beta, \eta, \sigma) = \lim_{n \to \infty} \theta_n(\beta, \eta, \sigma) = \sigma \frac{\lambda_0^{\beta - f_\Delta(\beta)}}{(\beta+1)\lambda_0 - \beta}, \tag{17}$$

where

$$f_\Delta(\beta) = \begin{cases} 2\eta & \text{if } 0 \le \beta \le \eta - \Delta, \\ \eta + \beta + \Delta & \text{if } \eta - \Delta \le \beta \le \eta + \Delta, \\ 2\beta & \text{if } \beta \ge \eta + \Delta. \end{cases} \tag{18}$$

Proof: From Rouché's theorem (see De Bruijn [7]) it readily follows that $\lambda_0 > |\lambda_j|$ for $j = 1, \dots, \beta$, and so from (7) we get

$$Z_i = c_0 \lambda_0^i \left(1 + o(1)\right), \quad i \to \infty. \tag{19}$$

Hence

$$\begin{aligned} &\lim_{n \to \infty} \theta_n(\beta, \eta, \sigma) \\ &= \lim_{n \to \infty} \sigma \frac{c_0 \lambda_0^{n-\max\{\beta,\eta-\Delta\}} c_0 \lambda_0^{n-\max\{\beta,\eta+\Delta\}}}{c_0 \lambda_0^{2n+1}} \\ &= \sigma c_0 \lambda_0^{-\max\{\beta,\eta-\Delta\}-\max\{\beta,\eta+\Delta\}-1}, \end{aligned} \tag{20}$$

which, using (8) with $j = 0$, yields (18). ■

Now that we have the limiting expression for the throughput in (17) we opt for an asymptotic analysis. That is, instead of searching for β_n^*, we search for its asymptotic counterpart

$$\beta^* = \operatorname*{argmax}_{\beta} \theta(\beta, \eta, \sigma), \tag{21}$$

where we henceforth consider θ as a function of the real variable $\beta \ge 0$. In Section III-B we show that the errors $|\theta_n - \theta|$ and $|\beta_n^* - \beta^*|$ become small, already for moderate values of n. Because we consider from here onwards the regime $n \to \infty$, all nodes have the same number of nodes within their sensing range. This removes all boundary effects, and all nodes have the same throughput, which is why just investigating node 0 is sufficient to investigate the entire network.

Proposition 4. $\beta^* \in [\eta - \Delta, \eta + \Delta]$.

The result of Proposition 4 can be understood as follows. By increasing β beyond $\eta + \Delta$, no additional collisions are prevented, but an increasing number of nodes is silenced. On the other hand, the nodes that become unblocked when decreasing β below $\eta-\Delta$, cause collisions when they activate. Although this result may seem intuitively clear, to the authors' knowledge such a result has not been proved rigourously (at least not in the present setting). Note that for all values $\beta \in [\eta-\Delta, \eta+\Delta]$, we can rewrite (17), using (6), as

$$\theta(\beta, \eta, \sigma) = g(\beta) \cdot \frac{(\lambda_0(\beta))^{\beta-\eta-\Delta}}{\beta+1} \tag{22}$$

with

$$g(\beta) = \frac{\lambda_0(\beta) - 1}{\lambda_0(\beta) - \frac{\beta}{\beta+1}} \to 1, \quad \beta \to \infty. \tag{23}$$

We are now in the position to present our main result. While we already know that the optimal sensing range is contained in the interval $[\eta-\Delta, \eta+\Delta]$, the next result is more specific.

Theorem 1. *There exists a threshold interval* $[\sigma_{\min}, \sigma_{\max}]$ *such that*

$$\beta^* = \begin{cases} \eta - \Delta & \text{if } \sigma \le \sigma_{\min}, \\ \eta + \Delta & \text{if } \sigma \ge \sigma_{\max}, \end{cases} \tag{24}$$

and β^* *increases from* $\eta-\Delta$ *to* $\eta+\Delta$ *when* σ *increases from* $\sigma_{\min}$ *to* $\sigma_{\max}$.

The proof of Theorem 1, see Section VI, follows from a detailed study of $\theta(\beta, \eta, \sigma)$ which involves implicit differentiation with respect to β (since $\lambda_0(\beta)$ is defined implicitly).

Theorem 1 can be interpreted as follows (see Figure 2). When σ is large, nodes activate very quickly after finishing their previous transmissions. When the system is in a maximal independent set, and if collisions are not ruled out, an activating node suffers a collision almost surely. This explains why for σ large, the optimal sensing range is $\beta = \eta + \Delta$, preventing collisions completely. On the other hand, when σ is small, collisions become rare, as few nodes are active simultaneously. In this case, the throughput is best served by increasing the spatial reuse, that is, decreasing the sensing range (up to $\eta - \Delta$). This explains the result of Theorem 1 for σ small.

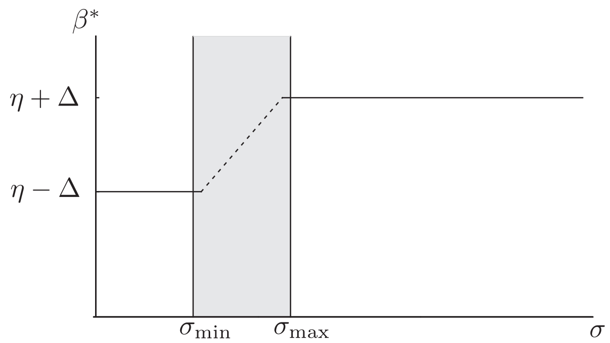

Fig. 2. The optimal sensing range β^* as a function of σ.

Note that Theorem 1 does not give the exact values of $\sigma_{\min}$ and $\sigma_{\max}$. Instead, we give below an estimate of the location and width of the threshold interval.

Theorem 2. *Let* $\kappa = \frac{\tau}{\eta+\Delta}$ *with* $\tau = (\sqrt{5}-1)/2$.
(i) The threshold interval is bounded as

$$[\sigma_{\min}, \sigma_{\max}] \subseteq [\kappa(1+\kappa)^{\eta-\Delta}, \kappa(1+\kappa)^{\eta+\Delta}]. \tag{25}$$

(ii) The width of the threshold interval is asymptotically given as

$$\sigma_{\max} - \sigma_{\min} \sim \frac{2e^{\tau}\Delta}{7+4\tau}\left(\frac{1}{\eta+1}\right)^2 \quad \text{as } \eta \to \infty. \tag{26}$$

Here we say that $f(\eta) \sim g(\eta)$ if $f(\eta)/g(\eta) \to 1$ as $\eta \to \infty$. From Theorem 2(ii) we see that the width of the threshold interval is $\mathcal{O}(\eta^{-2})$. Therefore, the interval width decreases rapidly as a function of η, and we can speak of an almost immediate transition from one regime ($\beta^* = \eta - \Delta$) to the other ($\beta^* = \eta + \Delta$). As a by-product of the proof of Theorem 2(ii) we obtain sharp approximations for $\sigma_{\min}$ and $\sigma_{\max}$, see (93)-(94):

$$\hat{\sigma}_{\min} = \hat{\mu}_-(1+\hat{\mu}_-)^{\eta-\Delta}, \quad \hat{\sigma}_{\max} = \hat{\mu}_+(1+\hat{\mu}_+)^{\eta+\Delta}, \tag{27}$$

with $\hat{\mu}_\pm = \tau/(\eta+\alpha_\pm)$ and $\alpha_\pm = ((2\Delta+3\pm 2\Delta)\tau + 2\Delta - 1)/2(2\tau+1)$.

So far we have maximized the throughput over β, while assuming σ to be fixed. We now assume σ is bounded as $0 < \sigma < \sigma_1$ for some constant σ_1, and consider the joint optimization problem of finding the (σ, β)-pair that solves

$$(\sigma, \beta)^* = \underset{\beta, 0<\sigma<\sigma_1}{\operatorname{argmax}}\, \theta(\beta, \eta, \sigma). \tag{28}$$

There is the following result.

Theorem 3. *The solution to the joint optimization problem* (28) *is given by*

$$(\sigma, \beta)^* = (\sigma_1, \beta^*(\sigma_1)). \tag{29}$$

So according to Theorem 3, the throughput is maximized by setting σ as large as possible, and choosing the corresponding optimal value of β.

A. Throughput limiting behavior

We now consider some limiting regimes for which we can make more explicit statements about the throughput. From Theorem 2 we can already see that the threshold interval moves in the direction of zero as η becomes large which implies that $\beta^* = \eta + \Delta$ for small values of σ. The next result shows that in the regime where η becomes large, the maximum throughput tends to zero.

Proposition 5. *Let* $\sigma > 0$ *be fixed. As* $\eta \to \infty$,

$$\max_{\beta} \theta(\beta, \eta, \sigma) = \frac{1}{\eta+\Delta+1}\left(1 + \mathcal{O}\left(\frac{1}{\ln(\eta+\Delta)}\right)\right). \tag{30}$$

For $\beta \ge \eta + \Delta$ our model reduces to a model without collisions that was studied extensively in [3], [5], [10], [22], [25], [28]. In particular, one immediately obtains from (6) and (17) the following result:

Corollary 1. *Let* $\beta \ge \eta + \Delta$. *Then*

$$\theta(\beta, \eta, \sigma) = \frac{\lambda_0 - 1}{(\beta+1)\lambda_0 - \beta}. \tag{31}$$

This result was also derived in [3], [10], [22], [28]. Note that as the intended receiver is no longer relevant in the case without collisions, Δ does not appear in (31).

From Proposition 7 and the proof of Proposition 5 it is seen that $\lambda_0 \to \infty$ as $\sigma \to \infty$ and β is fixed, and that $\beta(\lambda_0 - 1) \to \infty$ as $\beta \to \infty$ and σ is fixed. Thus the throughput is approximately $\frac{1}{\beta+1}$ when either σ or β is large. This can be understood as follows. For large σ, the high activation rate allows for configurations close to the maximum-size independent set: A configuration in which one out of every $\beta + 1$ nodes in active. For β large, when a node deactivates, a large number of neighboring nodes become eligible for activation. The time until the first such node activates goes to 0 when β increases.

Corollary 2. *Let $\beta < \eta + \Delta$. Then*

$$\lim_{\sigma \to \infty} \theta(\beta, \eta, \sigma) = 0. \tag{32}$$

Proof: From (45) with $j = 0$ it follows that

$$\lambda_0(\sigma) = \sigma^{\frac{1}{1+\beta}} + \mathcal{O}(1), \quad \sigma \to \infty. \tag{33}$$

Substituting (33) into (17), and using that $f_\Delta(\beta) > 2\beta$ when $\beta < \eta + \Delta$, yields

$$\begin{aligned} \theta(\beta, \eta, \sigma) &= \frac{\sigma(\sigma^{\frac{1}{1+\beta}} + \mathcal{O}(1))^{\beta - f_\Delta(\beta)}}{(\beta+1)(\sigma^{\frac{1}{1+\beta}} + \mathcal{O}(1)) - \beta} \\ &= \frac{1}{\beta+1}\sigma^{\frac{2\beta - f_\Delta(\beta)}{\beta+1}}(1 + o(1)) \to 0, \quad \sigma \to \infty, \end{aligned} \tag{34}$$

which gives (32). ■

Figure 3 shows the throughput plotted against the activation rate σ for $\eta = 7$, $\Delta = 1$ and various values of β. When $\beta \le \eta$, the throughput gradually drops to 0, whereas for $\beta \ge \eta + 1$, the throughput will eventually converge to the limit $1/(\beta+1)$. This confirms Corollaries 1 and 2.

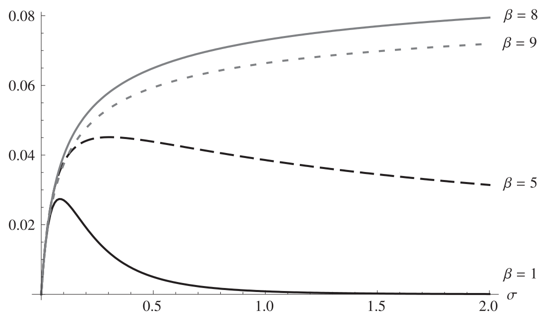

Fig. 3. The throughput $\theta(\beta, \eta, \sigma)$ plotted against σ for $\eta = 7$ and various values of β.

B. Finite versus infinite line networks

We now look at the approximation error $|\theta_n - \theta|$ and the resulting error in the optimal sensing range. To investigate the error we plot θ_n and θ in Figure 4, represented by the dashed line and the solid line, respectively. All results for θ_n were obtained by using (7) and (9) in combination with the infinite-series expressions for the roots in Section IV. In this section we restrict ourselves to the case $\Delta = 1$, but we see similar behavior for general Δ.

We take $n = 100$ (201 nodes), $\eta = 4$, and we let β increase from 1 to 100. In Figure 4(a) $\sigma = 0.25$, and in Figure 4(b) $\sigma = 5$. For β small the error $|\theta_n(\beta) - \theta(\beta)|$ is negligible, but the error increases as β increases. This can be explained by the observation that for larger β, the number of roots of (6) increases, as does the number of roots discarded by the approximation. This phenomenon becomes more pronounced for larger values of σ. The non-monotone behavior of θ_n is caused by the fact that for finite n, the system is directed to maximum-size independent sets of active nodes, in particular for σ large, and these sets change dramatically with β. The most important observation is that the error $|\theta_n - \theta|$ is small for those values of β that lead to a large throughput. Figure 5

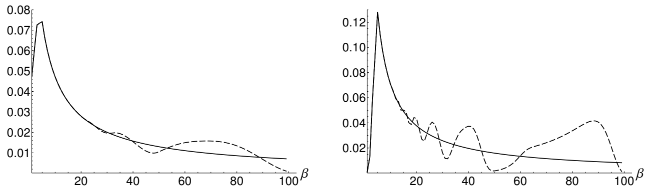

(a) $\sigma = 0.25$ (b) $\sigma = 5$

Fig. 4. The throughput θ_n (dashed) and θ (solid) plotted against β (with $n = 100$).

is similar to Figure 4, but instead of fixing n and varying β, we set $\beta = 16$ and vary n. In Figure 5(a) we take $\sigma = 0.25$ and in Figure 5(b) we take $\sigma = 5$. The accuracy of the approximation increases with n.

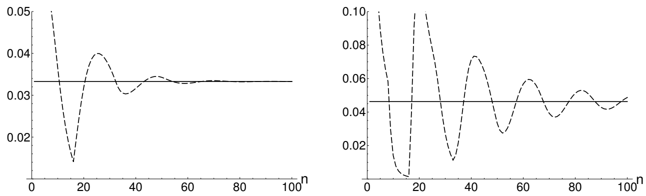

(a) $\sigma = 0.25$ (b) $\sigma = 5$

Fig. 5. The throughput θ_n (dashed) and θ (solid) plotted against n (with $\beta = 16$).

Figure 6 shows the optimal sensing range plotted against σ, for $\eta = 5$. Each of the Figures 6(a)-6(d) shows the optimal range $\beta_n^*(\sigma)$ for finite n. We take $\eta = 5$ for all figures, and let σ increase from 0.15 to 0.19. The vertical lines indicate the approximations of the threshold interval from (27), and we see that these are sharp. The optimal sensing range β^* for $n \to \infty$ behaves as predicted by Theorem 1, jumping from $\eta - 1$ before the threshold interval, to $\eta + 1$ after this interval, and β_n^* shows a similar pattern. We conclude that $n \to \infty$ provides a good approximation for the behavior of finite-sized networks, already for small and moderate values of n.

An alternative approach to studying the difference between finite and infinite networks is to look at the rate at which θ_n converges to θ. This rate is characterized by $|\lambda_1/\lambda_0|$, the modulus of the ratio of the second-largest and largest root of (6). Approximating λ_0 and λ_1 using the terms $l = 1, 2$ from the expansion (45), we obtain for σ large

$$\left|\frac{\lambda_1}{\lambda_0}\right| \approx (1 - 2r(1-r)(1 - \cos\alpha))^{1/2}, \tag{35}$$

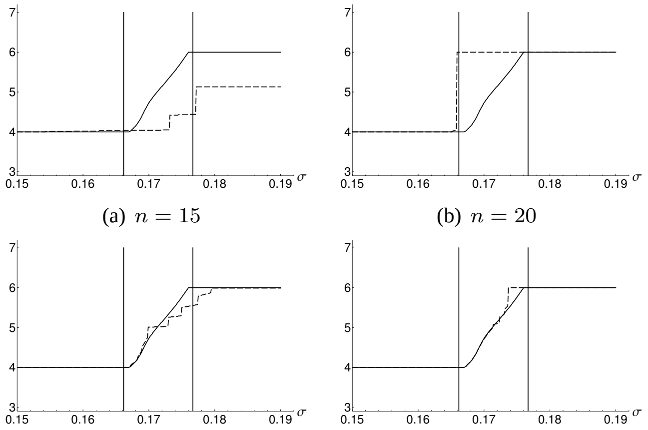

(a) $n = 15$ (b) $n = 20$

(c) $n = 25$ (d) $n = 30$

Fig. 6. The optimal sensing range β_n^* (dashed) and β^* (solid) plotted against σ around the threshold interval for various values of n and $\eta = 5$.

where

$$r = \frac{1}{(\beta+1)\sigma^{1/(\beta+1)}}, \quad \alpha = \frac{2\pi}{\beta+1}. \tag{36}$$

The case with σ small generally shows better convergence, as illustrated in Figure 5. Here a similar approximation can be obtained using (37) and (38).

IV. Partition function roots

In this section we study the roots $\lambda_0, \ldots, \lambda_\beta$ of (6) in more detail. In particular, we derive exact infinite-series expressions for the roots that are used in this paper both for numerical purposes (in Section V) and to prove Corollary 2. These roots are essential in Section III-B, where the finite and infinite networks are compared. Our main tool will be the Lagrange inversion theorem (see [7]), and depending on the value of σ, this gives two different infinite-series expressions. Let $(x)_n = \Gamma(x+n)/\Gamma(x)$ denote the Pochhammer symbol.

Proposition 6. *For small $\sigma > 0$,*

$$\lambda_0(\sigma) = 1 + \sum_{l=1}^{\infty} \frac{(-1)^{l-1}(\beta l)_{l-1}}{l!}\sigma^l, \tag{37}$$

$$\lambda_j(\sigma) = \sum_{l=1}^{\infty} \frac{(l/\beta)_{l-1}}{l!} w_j^l, \quad j = 1, 2, \ldots, \beta, \tag{38}$$

where $w_j = \sigma^{1/\beta} \mathrm{e}^{2\pi\imath(j-1/2)/\beta}$ and $\imath = \sqrt{-1}$. The series expansions in (37) *and* (38) *converge for*

$$0 \le \sigma \le \frac{\beta^\beta}{(\beta+1)^{\beta+1}} =: \xi(\beta), \tag{39}$$

and diverge otherwise.

Proof: We first consider the case $j = 0$. Set $\mu_0 = \lambda_0 - 1$, so μ_0 satisfies $\mu_0(1+\mu_0)^\beta = \sigma$. Hence for small values of $|\sigma|$ we have by Lagrange's inversion theorem

$$\begin{aligned} \mu_0 &= \sum_{l=1}^{\infty} \frac{1}{l!}\left(\frac{\mathrm{d}}{\mathrm{d}\mu}\right)^{l-1} \left[\left(\frac{\mu}{\mu(1+\mu)^\beta}\right)^l\right]_{\mu=0} \sigma^l \\ &= \sum_{l=1}^{\infty} \frac{(-1)^{l-1}(\beta l)_{l-1}}{l!}\sigma^l. \end{aligned} \tag{40}$$

Next we consider the case that $j = 1, \ldots, \beta$. We now write (6) as

$$\lambda^\beta(1-\lambda) = -\sigma, \quad \lambda(1-\lambda)^{1/\beta} = w_j, \tag{41}$$

where

$$w_j = \sigma^{1/\beta}\mathrm{e}^{2\pi\imath(j-1/2)/\beta}. \tag{42}$$

Then we get for $|w_j|$ sufficiently small

$$\begin{aligned} \lambda_j &= \sum_{l=1}^{\infty} \frac{1}{l!}\left(\frac{\mathrm{d}}{\mathrm{d}\lambda}\right)^{l-1} \left[\left(\frac{\lambda}{\lambda(1-\lambda)^{1/\beta}}\right)^l\right]_{\lambda=0} w_j^l \\ &= \sum_{l=1}^{\infty} \frac{(l/\beta)_{l-1}}{l!} w_j^l. \end{aligned} \tag{43}$$

The radii of convergence of the series in (40) and (43) are easily obtained from the asymptotics

$$\Gamma(x+1) = x^{x+1/2}\mathrm{e}^{-x}\sqrt{2\pi}(1+\mathcal{O}(x^{-1})), \quad x \to \infty, \tag{44}$$

of the Γ-function, used to examine the Pochhammer quantities $(x)_n = \Gamma(x+n)/\Gamma(x)$ and the factorials $l! = \Gamma(l+1)$ that occur in both series. This yields the result that both series converge when $|\sigma| \le \xi(\beta)$ and diverge for $|\sigma| > \xi(\beta)$. When $|\sigma| = \xi(\beta)$ the terms in either series are $\mathcal{O}(l^{-3/2})$. ∎

Proposition 7. *For large $\sigma > 0$,*

$$\lambda_j(\sigma) = \left(\sum_{l=1}^{\infty} \frac{\left(\frac{-l}{\beta+1}\right)_{l-1}}{l!} v_j^{-l}\right)^{-1}, \quad j = 0, 1, \ldots, \beta, \tag{45}$$

where $v_j = \sigma^{1/(\beta+1)}\mathrm{e}^{2\pi\imath j/(\beta+1)}$. The series expansion in (45) *converges for*

$$\sigma \ge \xi(\beta), \tag{46}$$

and diverges otherwise, where $\xi(\beta)$ is given in (39).

Proof: We can treat the cases $j = 0$ and $j = 1, \ldots, \beta$ simultaneously now. We write (6) in the form

$$\frac{1}{\lambda}\left(1 - \frac{1}{\lambda}\right)^{\frac{-1}{\beta+1}} = \left(\frac{1}{\sigma}\right)^{\frac{1}{\beta+1}} = v^{-1}, \tag{47}$$

where we let

$$v^{-1} = v_j^{-1} = \left(\frac{1}{\sigma}\right)^{\frac{1}{\beta+1}} \mathrm{e}^{-2\pi\imath\frac{j}{\beta+1}}, \quad j = 0, 1, \ldots, \beta \tag{48}$$

with $\sigma^{-\frac{1}{\beta+1}} > 0$ in (48). We get for sufficiently large σ from Lagrange's inversion theorem (with $u = 1/\lambda$) that

$$\begin{aligned} \frac{1}{\lambda_j} &= \sum_{l=1}^{\infty} \frac{1}{l!}\left(\frac{\mathrm{d}}{\mathrm{d}u}\right)^{l-1} \left[\left(\frac{u}{u(1-u)^{-1/(\beta+1)}}\right)^l\right]_{u=0} v_j^{-l} \\ &= \sum_{l=1}^{\infty} \left(\frac{-l}{\beta+1}\right)_{l-1} \frac{v_j^{-l}}{l!}. \end{aligned} \tag{49}$$

The Pochhammer quantity $(\frac{-l}{\beta+1})_{l-1}$ vanishes if and only if $l = 1, 2, \ldots$ is a multiple of $\beta + 1$. The radius of convergence of the series in (49) is again determined by the asymptotics of the Γ-function in (44). Here it must also be used that

$$\Gamma(-J) = \frac{-1}{\Gamma(J+1)}\frac{\pi}{\sin \pi J}, \quad J > 0. \tag{50}$$

It follows that the series in (49) is convergent when $|\sigma| \geq \xi(\beta)$ and divergent when $|\sigma| < \xi(\beta)$. When $|\sigma| = \xi(\beta)$ the terms in the series are $\mathcal{O}(l^{-3/2})$. ∎

Figure 7 shows the roots of (6) drawn in the complex λ-plane for $\beta = 4$. Each heavy solid line corresponds to a root as a function of σ, and the dots represent the threshold $|\sigma| = \xi(\beta)$. The light solid straight line and the dashed straight line illustrate the leading behavior of each root as $\sigma \downarrow 0$ or $\sigma \to \infty$ according to Propositions 6 and 7, respectively. The dashed curve encircling the origin 0 and the point 1 is the image of $v \in \mathbb{C}$ with $|v| = \sigma^{1/(\beta+1)}$, $\sigma = \xi(\beta)$, under the mapping given by the reciprocal of the right-hand side of (45) with v_j replaced by v.

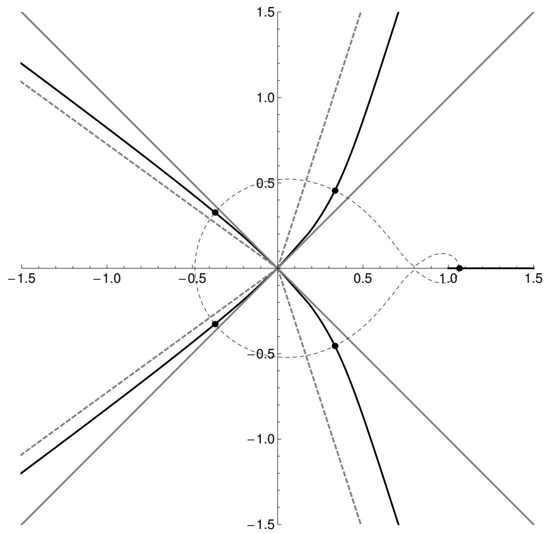

Fig. 7. The roots of $\lambda^{\beta+1} + \lambda^{\beta} = \sigma$ as functions of σ in (37), (38) and (45), for $\beta = 4$.

V. Discussion and outlook

The distinguishing feature of this paper is the presence of node interaction when making the tradeoff between hidden nodes and exposed nodes. In order to get a handle on the throughput function (and hence the partition function) we studied the wireless network in the asymptotic regime of infinitely many nodes. This resulted in a tractable limiting expression for the throughput of node zero (and hence of any other node) that allowed us to prove the following three results:

(i) To optimize the throughput, one should always choose a sensing range β that is close to the interference range η, and in fact the optimal sensing range is contained in the interval $[\eta - \Delta, \eta + \Delta]$ (see Proposition 4).

(ii) The sensing range β^* that optimizes the throughput equals $\eta - \Delta$ for less aggressive nodes (small σ) and $\eta + \Delta$ for aggressive nodes (large σ). In fact, we were able to show the existence of a threshold interval for σ that distinguishes these two regimes (Theorem 1). This important result provides (partial) justification for the frequently made assumption that no collisions occur. Indeed, one key take away is that if σ is large enough, ruling out all collisions by setting $\beta = \eta + \Delta$ is optimal.

(iii) In case the σ can take any value $0 \leq \sigma \leq \sigma_1$, the pair $(\sigma, \beta)^*$ that jointly maximizes the throughput is given by $(\sigma_1, \beta^*(\sigma_1))$. So the optimal setting is to choose the σ as large as possible, and then to select the sensing range that maximizes throughput for this particular σ-value.

We have further shown that the threshold interval is in many cases small, which implies that one can speak of an almost immediate transition from one regime ($\beta^* = \eta - \Delta$) to the other ($\beta^* = \eta + \Delta$). We have argued that, when the aggressiveness of the nodes is large enough, the system no longer gains from the potential benefits of more flexibility (small β), and just settles for the situation with no collisions.

We shall now discuss two remaining issues. In Section V-A we consider the case of random transmission distance, and in Section V-B we investigate whether the notions of two regimes and a critical threshold carry over to more general topologies.

A. Random transmission distance

We now relax the assumption that packets are always sent to nodes at distance Δ, and instead allow for transmissions towards any node within some transmission range $D \geq 1$. We assume that a transmission is intended for a node at distance Δ with probability a_Δ, $\Delta = 1, \ldots, D$. By conditioning on the transmission distance and following the arguments from the proof of Proposition 2, the throughput $\hat{\theta}_n$ in this case may be written as

$$\hat{\theta}_n(\beta, \eta, \sigma) = \sum_{\Delta=1}^{D} a_\Delta \sigma \frac{Z_{n-\max\{\beta,\eta-\Delta\}} Z_{n-\max\{\beta,\eta+\Delta\}}}{Z_{2n+1}}, \tag{51}$$

with Z_i the partition function (7), as before.

The choice for sensing range $\hat{\beta}_n$ that maximizes (51) behaves markedly different from the fixed-range case. Consider for example a network with $n = 15$, $\eta = 6$ and $D = 2$ (so the transmission range is either 1 or 2). We numerically compute the $\hat{\beta}_n$ as a function of σ for $a_1 = 0.1$ and $a_2 = 0.9$ (Figure 8(a)) and for $a_1 = 0.7$ and $a_2 = 0.3$ (Figure 8(b)). The optimal sensing range no longer consists of two regimes separated by a threshold interval, and we see that $\hat{\beta}_n$ does not necessarily approach $\eta + D = 8$ when σ is large. This can be explained by the observation that, for σ large, the contribution to the throughput by transmissions over a distance of at least $\beta - \eta$ will approach 0, since the network is so densely packet that all such transmission will suffer a collision. However, transmissions over a smaller distance will remain successful, so depending on the choice of the a_Δ, it might be beneficial to choose a sensing range that is smaller than $\eta + D$, even for $\sigma \to \infty$.

Analogous to Proposition 3, when the network becomes large we can once more use the asymptotic in (7), and we may write

$$\hat{\theta}(\beta, \eta, \sigma) = \lim_{n\to\infty} \hat{\theta}_n(\beta, \eta, \sigma) = \sum_{\Delta=1}^{D} a_\Delta \theta_\Delta(\beta, \eta, \sigma), \tag{52}$$

with

$$\theta_\Delta(\beta, \eta, \sigma) = \sigma \frac{\lambda_0^{\beta - f_\Delta(\beta)}}{(\beta+1)\lambda_0 - \beta}. \tag{53}$$

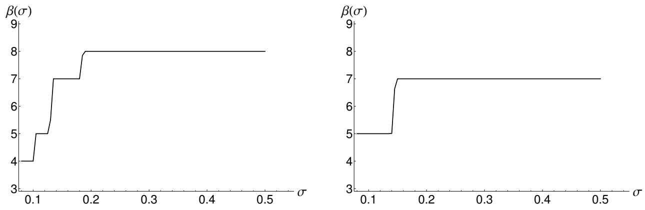

(a) $\xi_1 = 0.1$ and $\xi_2 = 0.9$

(b) $\xi_1 = 0.7$ and $\xi_2 = 0.3$

Fig. 8. The impact of the sensing range as a function of σ, for $\eta = 6$, $D = 2$ and $n = 15$.

This asymptotic throughput function may have several stationary points as a function of β, as is illustrated in Figure 9. This makes the issue of finding an optimal $\beta^*(\sigma)$ more complicated than in the case of a fixed transmission range.

Although each of the individual terms θ_Δ in (52) has a unique stationary point, there is no intuitive explanation why uniqueness does not necessarily hold when multiple terms are combined. It is worth noting that the existence of multiple stationary points appears rare, and that the counterexample for uniqueness in Figure 9 relies on the careful choice for the coefficients a_1 and a_2.

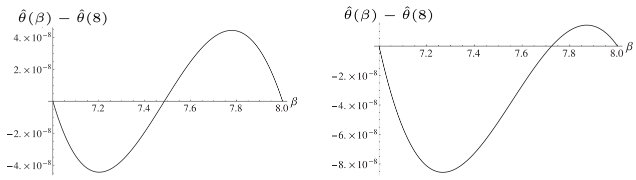

(a) $\sigma = 0.204$

(b) $\sigma = 0.205$

Fig. 9. $\hat{\theta}(\beta, \eta, \sigma) - \hat{\theta}(8, \eta, \sigma)$ plotted against $\beta \in [7, 8]$, for $\eta = 6$, $\Delta = 2$, $a_1 = 0.132$, $a_2 = 0.868$ and various values of σ.

B. General topologies

In order to investigate topologies beyond linear networks we require a more general description of the model. In addition to nodes we also introduce links connecting two nodes, representing the possibility of transmissions taking place between these nodes. For two nodes to be able to transmit data, we require them to be at most within (Euclidian) distance d of each other, and we assume that links are formed between all nodes within distance d. Each node has activation rate σ, and the destination of a transmission is chosen uniformly among all links originating from the activating node. The sensing range β and interference range η are also defined using Euclidian distance.

Our numerical experiments consist of discrete-event simulations of the dynamics described in Section II, generalized to arbitrary network topologies. While for infinite line networks it suffices to maximize the throughput of just node 0 (due to symmetry), our objective for general networks is to maximize the average per-node throughput. First, we apply this objective to a 16-node linear network with nodes at unit distance and $d = 1$, so nodes only transmit to direct neighbors. Figure 10 shows the optimal sensing range β^* as a function of σ, for $\eta = 2$ and $\eta = 4$. We see that β^* behaves similar to the optimal sensing range for finite linear networks observed in Section III-B, which suggests that using the average throughput as an objective is a natural extension of the throughput of node 0. Most importantly, we observe the anticipated dependence of β^* on σ, and a very narrow critical interval between the regimes β^* small and β^* large.

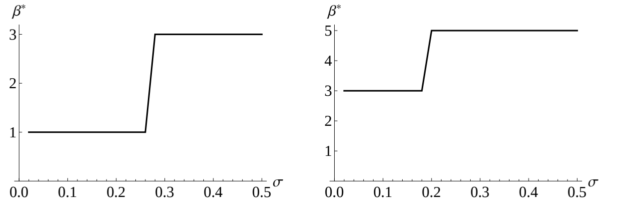

(a) $\eta = 2$

(b) $\eta = 4$

Fig. 10. The throughput-average optimal sensing range for a 16-node linear network.

Next we consider 16 nodes placed on a 4×4 grid at unit distance from each other. We set $d = 1$ and $\eta = 1$, so each node is connected with up to 4 links, and transmissions are potentially interfered with by activity of the direct neighbors of the receiving node, see Figure 11(a). Figure 11(b) shows the optimal sensing range β^* plotted against σ. Similar to our analytical results for the linear network we observe that σ has a significant impact on the optimal sensing range: The β^* is increasing in σ. The intuition for this is similar to that for linear networks provided in Section III. Note that the two optimal regimes are once again separated by a narrow critical interval.

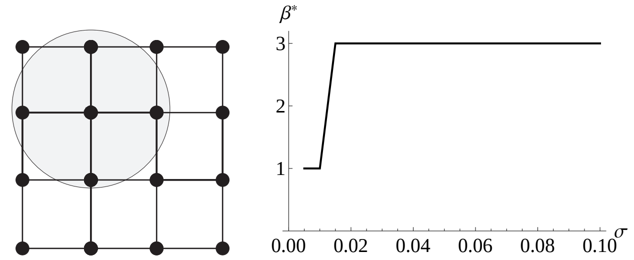

(a) A 4×4 grid network.

(b) The optimal sensing range β^* plotted against σ.

Fig. 11. A grid network and its optimal sensing range.

Finally, we obtain by simulation the optimal sensing range for two randomly generated networks. Each network is created by placing 16 nodes uniformly at random in a unit square. We assume a transmission range of $d = 0.2$ and interference range $\eta = 0.4$. Figure 12 shows the topologies of both networks under consideration: The vertices correspond to the nodes and two nodes share an edge if they are within transmission range $d = 0.2$. We let the sensing range vary from $\beta = 0$ to $\beta = 0.5$ in small increments, and simulate for each β the throughput as a function of σ. Figure 13 shows the average per-node throughput plotted against σ, for various values of β, and in Figure 14 we plot the optimal sensing range β^* obtained from the simulations.

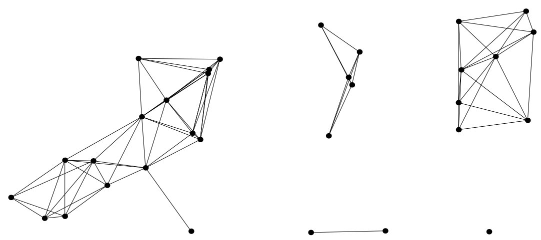

(a) Network 1 (b) Network 2

Fig. 12. Two heterogeneous network topologies.

The two irregular networks shown in Figure 12 have very distinct structures, and as expected the behavior and performance of CSMA differs significantly between these networks. Compare for example the difference in throughput, and the fact that the impact of the sensing range is smaller for network 2. However, both networks also show striking similarities, and behave largely as predicted by our analytical results for linear networks. For instance, we see that for β small, the throughput drops as σ increases due to the higher number of collisions. Moreover, the optimal sensing range β^* is an increasing function of σ. Note that for these particular networks the existence of various optimal regimes separated by critical intervals is less pronounced. In general, the tradeoff for individual nodes in an irregular network is more complex than in a linear network due to the node heterogeneity, and raises many interesting questions for future research.

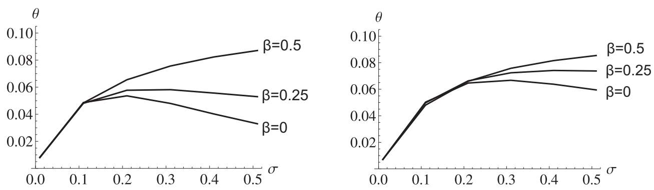

(a) Network 1 (b) Network 2

Fig. 13. The throughput for various values of β.

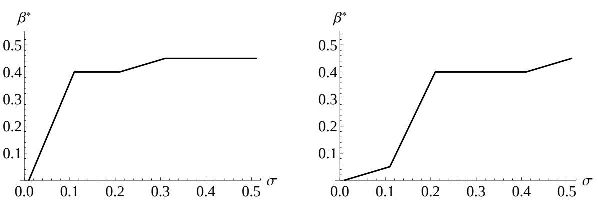

(a) Network 1 (b) Network 2

Fig. 14. The optimal sensing range plotted against σ.

C. *Future work*

Wireless networks equipped with CSMA on complex topologies form highly relevant objects for further study. In particular, we have raised the question whether a threshold interval for the activation rate σ exists, which says that the optimal sensing ranges equals β_L for σ below the interval, and β_U for σ above the interval. For the two examples in Section V-B there is indeed such a threshold interval, but a more thorough study is needed.

Obtaining numerical and analytical results for complex topologies with many nodes is challenging. For one thing, the state space no longer decomposes (as with the line network), so that the calculation of the partition function becomes more involved. In determining the stationary distribution, and hence the throughput of nodes, the brute-force method would be to sum over all possible configurations, but that will become computationally cumbersome, already for moderate instances of the network. Alternative approaches would be to use limit theorems, for instance for highly dense networks with many nodes. We conjecture that in such networks we would again find that the optimal sensing range is increasing rather than constant in the activation rate.

VI. Remaining proofs

A. *Proof of Proposition 1*

We write the generating function from (5) as

$$Z(x,\sigma)=\frac{P(x)}{S(x)}, \tag{54}$$

where

$$P(x)=1+\sigma\frac{x^{\beta+1}-x}{x-1}, \quad S(x)=1-x-\sigma x^{\beta+1}. \tag{55}$$

It is shown in [22] that the equation $S(x)=0$ has $\beta+1$ roots x_j, $j=0,1,\ldots,\beta$, and exactly one of them, x_0 is real and positive, while $|x_j|>x_0$, $j=1,\ldots,\beta$. To prove Proposition 1 we first need to establish that these roots are distinct.

Proposition 8. *The roots of $S(x)=0$ are distinct.*

Proof: When $S(x)=S'(x)=0$, we have

$$1-x-\sigma x^{\beta+1}=0=-1-\sigma(\beta+1)x^{\beta}. \tag{56}$$

This implies that $x=1+\frac{1}{\beta}>1$ and so that $\sigma=\frac{1-x}{x^{\beta+1}}<0$. However, σ is non-negative. ■

Now we proceed with the proof of Proposition 1. Let $\lambda_j=1/x_j$ so that $\lambda=\lambda_j$ satisfies (6). Using that all zeros of S are distinct, we have for $Z(x,\sigma)$ the partial fraction expansion

$$Z(x,\sigma)=\sum_{j=0}^{\beta}\frac{P(x_j)}{S'(x_j)}\frac{1}{x-x_j}. \tag{57}$$

Now

$$\begin{aligned}\frac{P(x_j)}{S'(x_j)}&=\frac{1+\sigma\frac{x_j^{\beta+1}-x_j}{x_j-1}}{-1-(\beta+1)\sigma x_j^{\beta}}=\frac{-x_j^{-\beta}}{1+(\beta+1)\sigma x_j^{\beta}}\\&=\frac{-x_j^{-\beta}}{1+(\beta+1)\frac{1-x_j}{x_j}}=\frac{-\lambda_j^{\beta}}{(\beta+1)\lambda_j-\beta}.\end{aligned} \tag{58}$$

Here it has been used that

$$\frac{1}{1-x_j}=\frac{-1}{\sigma x_j^{\beta+1}}, \quad \sigma x_j^{\beta}=\frac{1-x_j}{x_j}. \tag{59}$$

Then for $|x| < x_0$ we have

$$Z(x,\sigma) = \sum_{j=0}^{\beta} \frac{P(x_j)}{S'(x_j)} \sum_{i=0}^{\infty} \frac{-x^i}{x_j^{i+1}}$$
$$= \sum_{i=0}^{\infty} x^i \left(\sum_{j=0}^{\beta} \frac{\lambda_j^{\beta+1}}{(\beta+1)\lambda_j - \beta} \lambda_j^i \right), \qquad (60)$$

as required.

B. Proof of Proposition 4

As introduced earlier,

$$\mu_0 = \lambda_0 - 1. \qquad (61)$$

Then μ_0 depends on β and σ, we have $\mu_0 > 0$, and

$$\mu_0(1+\mu_0)^{\beta} = \sigma. \qquad (62)$$

By implicit differentiation with respect to β, we get from (62) that

$$\frac{\partial \mu_0}{\partial \beta} = \frac{-\mu_0(1+\mu_0)\ln(1+\mu_0)}{1+\mu_0+\beta\mu_0}. \qquad (63)$$

In particular, both μ_0 and λ_0 decrease as a function of $\beta > 0$.

Consider the case that $0 \le \beta \le \eta - 1$. Using $\lambda_0^{\beta} = \frac{\sigma}{\lambda_0 - 1}$ we get

$$\theta(\beta,\eta,\sigma) = \sigma^2 \frac{\lambda_0^{-2\eta}}{(\lambda_0-1)((\beta+1)\lambda_0 - \beta)}$$
$$= \sigma^2 \frac{\lambda_0^{-2\eta}}{\mu_0(1+\mu_0+\beta\mu_0)}. \qquad (64)$$

Now $\lambda_0^{-2\eta}$ increases as a function of β, and we shall show that $\mu_0(1+\mu_0+\beta\mu_0)$ decreases in $\beta > 0$. We have from (63) that

$$\frac{\partial}{\partial\beta}[\mu_0(1+\mu_0+\beta\mu_0)] = \frac{\partial}{\partial\beta}[\beta\mu_0^2 + \mu_0 + \mu_0^2]$$
$$= \mu_0^2 - \frac{1+2(1+\beta)\mu_0}{1+\mu_0+\beta\mu_0}\mu_0(1+\mu_0)\ln(1+\mu_0)$$
$$\le \mu_0(\mu_0 - (1+\mu_0)\ln(1+\mu_0)) < 0, \qquad (65)$$

where the last inequality follows from $x\ln x > x-1, x > 1$. We conclude that θ increases as a function of $\beta \in (0, \eta-1]$.

Next we consider the case that $\beta \ge \eta+1$. From $\lambda_0^{\beta} = \frac{\sigma}{\lambda_0 - 1}$ we get

$$\theta(\beta,\eta,\sigma) = \sigma \frac{\lambda_0^{-\beta}}{(\beta+1)\lambda_0 - \beta} = \frac{\lambda_0 - 1}{(\beta+1)\lambda_0 - \beta}$$
$$= \frac{\mu_0}{1+\mu_0+\beta\mu_0}. \qquad (66)$$

Now

$$\frac{\partial}{\partial\beta}\left(\frac{\mu_0}{1+\mu_0+\beta\mu_0}\right) = \frac{\frac{\partial\mu_0}{\partial\beta} - \mu_0^2}{(1+\mu_0+\beta\mu_0)^2} < 0, \qquad (67)$$

see (63), and so θ decreases as a function of $\beta \ge \eta+1$. Since θ depends continuously on $\beta > 0$, the result follows.

C. Proof of Theorem 1

The proof of the result as stated in Theorem 1 requires expanding several other results. We consider $\beta \in [\eta-\Delta, \eta+\Delta]$ so that

$$\theta(\beta,\eta,\sigma) = \sigma \frac{\lambda_0^{-\eta-\Delta}}{(\beta+1)\lambda_0 - \beta} = \sigma \frac{(1+\mu_0)^{-\eta-\Delta}}{1+\mu_0+\beta\mu_0}. \qquad (68)$$

From (63) it follows from a straightforward but somewhat lengthy computation that

$$\frac{\partial}{\partial\beta}[\theta(\beta,\eta,\sigma)] = \frac{-\sigma\mu_0(1+\mu_0)^{-\eta-\Delta}}{(1+\mu_0+\beta\mu_0)^2}$$
$$\times \left(1 - (\eta+\Delta+1+\frac{\beta}{1+\mu_0+\beta\mu_0})\ln(1+\mu_0)\right). \qquad (69)$$

Let

$$F(\beta,\sigma) = (\eta+\Delta+1+\frac{\beta}{1+\mu_0+\beta\mu_0})\ln(1+\mu_0). \qquad (70)$$

Then we have for $\beta \in [\eta-\Delta, \eta+\Delta]$ that

$$F(\beta,\sigma) > 1 \Rightarrow \theta \text{ increases strictly at } \beta, \qquad (71)$$
$$F(\beta,\sigma) < 1 \Rightarrow \theta \text{ decreases strictly at } \beta. \qquad (72)$$

We analyze $F(\beta,\sigma)$ in some detail, especially for values of β,σ such that $F(\beta,\sigma) = 1$. We recall here that $\mu_0 = \mu_0(\beta,\sigma)$ is a function of β and σ as well.

We fix $\beta > 0$, and we compute

$$\frac{\partial}{\partial\sigma}F(\beta,\sigma) = \left[\frac{\eta+\Delta}{\mu_0+1} + \frac{1+\beta}{1+\mu_0+\beta\mu_0} - \frac{\beta(1+\beta)\ln(1+\mu_0)}{(1+\mu_0+\beta\mu_0)^2}\right]\frac{\partial\mu_0}{\partial\sigma}. \qquad (73)$$

We get from (62) by implicit differentiation that

$$\frac{\partial\mu_0}{\partial\sigma} = \frac{\mu_0(1+\mu_0)}{\sigma(1+\mu_0+\beta\mu_0)} > 0. \qquad (74)$$

Furthermore, it is seen from (62) that $\mu_0(\beta,\sigma) \to 0$ as $\sigma \downarrow 0$ and that $\mu_0(\beta,\sigma) \to \infty$ as $\sigma \to \infty$. Hence, $\mu_0(\beta,\sigma)$ increases from 0 to ∞ as σ increases from 0 to ∞. Moreover,

$$\frac{\eta+\Delta}{\mu_0+1} > 0, \quad 1 > \frac{\beta\ln(1+\mu_0)}{1+\mu_0+\beta\mu_0}. \qquad (75)$$

It follows from (74) and (75) that $\frac{\partial}{\partial\sigma}F(\beta,\sigma) > 0$. Then, from (70) and from the fact that μ_0 increases from 0 to ∞ as σ increases from 0 to ∞, we have that $F(\beta,\sigma)$ increases from 0 to ∞ as σ increases from 0 to ∞. Therefore, for any $\beta > 0$, there is a unique $\sigma = \sigma(\beta)$ such that

$$F(\beta,\sigma) = F(\beta,\sigma(\beta)) = 1. \qquad (76)$$

We shall next show that $\sigma(\beta)$ increases in $\beta \in [\eta-\Delta, \eta+\Delta]$. By implicit differentiation in (76), we have for $\beta \in [\eta-\Delta, \eta+\Delta]$

$$0 = \frac{\mathrm{d}}{\mathrm{d}\beta}[F(\beta,\sigma(\beta))] = F_{\beta}(\beta,\sigma(\beta)) + \sigma'(\beta)F_{\sigma}(\beta,\sigma(\beta)), \qquad (77)$$

where F_{β} and F_{σ} denote the respective partial derivatives (and $\sigma'(\eta\pm\Delta)$ is the left and right derivative for $+$ and $-$, respectively). We already know that $F_{\sigma} > 0$, and we shall show now that $F_\beta(\beta,\sigma(\beta))<0$. To that end, we compute, using definition (70) of F and (63) that

$$\begin{aligned}&\frac{\partial}{\partial\beta}[F(\beta,\sigma)]\\ &= -\ln(1+\mu_0)\Big[(\eta+\Delta+1+\frac{\beta}{1+\mu_0+\beta\mu_0})\\ &\quad\times\frac{\mu_0}{1+\mu_0+\beta\mu_0}-\frac{1+\mu_0-\beta(1+\beta)\frac{\partial\mu_0}{\partial\beta}}{(1+\mu_0+\beta\mu_0)^2}\Big].\end{aligned}\tag{78}$$

Next, from (70) and (76) we have that

$$\mu_0\geq\ln(1+\mu_0)=\frac{1}{\eta+\Delta+1+\frac{\beta}{1+\mu_0+\beta\mu_0}},\tag{79}$$

and so

$$\begin{aligned}&\frac{\partial F}{\partial\beta}(\beta,\sigma(\beta))\leq-\ln(1+\mu_0)\\ &\quad\times\left[\frac{1}{1+\mu_0+\beta\mu_0}-\frac{1+\mu_0-\beta(1+\beta)\frac{\partial\mu_0}{\partial\beta}}{(1+\mu_0+\beta\mu_0)^2}\right]_{\sigma=\sigma(\beta)}\\ &=\frac{-\beta\ln(1+\mu_0)}{(1+\mu_0+\beta\mu_0)^2}\left[\mu_0+(1+\beta)\frac{\partial\mu_0}{\partial\beta}\right]_{\sigma=\sigma(\beta)}\\ &=\frac{-\mu_0\beta\ln(1+\mu_0)}{(1+\mu_0+\beta\mu_0)^2}\\ &\quad\times\left[1-(1+\beta)\frac{(1+\mu_0)\ln(1+\mu_0)}{1+\mu_0+\beta\mu_0}\right]_{\sigma=\sigma(\beta)},\end{aligned}\tag{80}$$

where (63) has been used once more. Finally, from (70) and (76),

$$\begin{aligned}&(1+\beta)\frac{(1+\mu_0)\ln(1+\mu_0)}{1+\mu_0+\beta\mu_0}\Big|_{\sigma=\sigma(\beta)}\\ &=\frac{(1+\beta)(1+\mu_0)}{(\eta+\Delta+1)(1+\mu_0+\beta\mu_0)+\beta}\Big|_{\sigma=\sigma(\beta)}<1,\end{aligned}\tag{81}$$

since $0<\beta\leq\eta+\Delta$ and $\mu_0>0$. Hence, $F_\beta(\beta,\sigma(\beta))<0$ as required. It now follows from (77) and from $F_\sigma(\beta,\sigma(\beta))>0$ that $\sigma'(\beta)>0$ when $\beta\in[\eta-\Delta,\eta+\Delta]$.

We have now shown that $\sigma(\beta)$ increases in $\beta\in[\eta-\Delta,\eta+\Delta]$. Next we let

$$\sigma_{\min}:=\sigma(\eta-\Delta)<\sigma(\eta+\Delta)=:\sigma_{\max}.\tag{82}$$

For $\sigma\in[\sigma_{\min},\sigma_{\max}]$ there is defined the inverse function $\beta(\sigma)\in[\eta-\Delta,\eta+\Delta]$ that increases in σ. It follows then from

$$F(\beta(\sigma),\sigma)=1,\quad F_\beta(\beta(\sigma),\sigma)<0\tag{83}$$

and (69)-(72) that $\theta(\beta,\eta,\sigma)$ is maximal at $\beta=\beta(\sigma)$ when $\sigma\in[\sigma_{\min},\sigma_{\max}]$.

We shall now complete the proof of Theorem 1. Let $\beta\in[\sigma_{\min},\sigma_{\max}]$, and assume that $\sigma\leq\sigma_{\min}$. Then $\sigma<\sigma(\beta)$ and so $F(\beta,\sigma)<F(\beta,\sigma(\beta))=1$ since F increases in σ. Hence, θ strictly decreases at β. Similarly, θ strictly increases at $\beta\in(\eta-\Delta,\eta+\Delta)$ when $\sigma\geq\sigma_{\max}$. It follows that θ strictly decreases in $\beta\in[\eta-\Delta,\eta+\Delta]$ when $\sigma\leq\sigma_{\min}$ and that θ strictly increases in $\beta\in[\eta-\Delta,\eta+\Delta]$ when $\sigma\geq\sigma_{\max}$. Finally, when $\sigma\in(\sigma_{\min},\sigma_{\max})$, we have that

$$\begin{aligned}&F(\eta-\Delta,\sigma)>F(\eta-\Delta,\sigma_{\min})\\ &\qquad=1=F(\eta+\Delta,\sigma_{\max})>F(\eta+\Delta,\sigma),\end{aligned}\tag{84}$$

showing that θ strictly increases at $\beta=\eta-\Delta$ and strictly decreases at $\beta=\eta+\Delta$, and assumes its maximum at $\beta=\beta(\sigma)$.

D. Proof of Theorem 2

We shall show below that

$$\begin{aligned}&(\eta+\Delta+1+\frac{\eta-\Delta}{1+(\eta-\Delta+1)\kappa})\ln(1+\kappa)<1\\ &\quad<(\eta+\Delta+1+\frac{\eta+\Delta}{1+(\eta+\Delta+1)\kappa})\ln(1+\kappa)\end{aligned}\tag{85}$$

where $\kappa=\tau/(\eta+\Delta)$. Assuming this, we recall that (for fixed $\beta>0$) μ_0 strictly increases in σ and vice versa. When now

$$\sigma_-=\kappa(1+\kappa)^{\eta-\Delta},\tag{86}$$

then $\kappa=\mu_0(\beta=\eta-\Delta,\sigma_-)$ and we have that $F(\eta-\Delta,\sigma_-)<1$. So $\sigma_-<\sigma_{\min}$ since F is increasing in σ. Similarly, when

$$\sigma_+=\kappa(1+\kappa)^{\eta+\Delta},\tag{87}$$

we have that $\kappa=\mu_0(\beta=\eta+\Delta,\sigma_+)$ and then from (85) that $F(\eta+\Delta,\sigma_+)>1$ and so $\sigma_+>\sigma_{\max}$.

This proves Theorem 2(i). It remains to show (85). As to the first inequality in (85) we have

$$\begin{aligned}&1-(\eta+\Delta+1+\frac{\eta-\Delta}{1+(\eta-\Delta+1)\kappa})\ln(1+\kappa)\\ &>1-(\eta+\Delta+1+\frac{\eta-1}{1+(\eta-\Delta+1)\kappa})\kappa\\ &=\frac{1}{1+(\eta-\Delta+1)\kappa}(1-(\eta+\Delta)\kappa-\eta(\eta+\Delta+1)\kappa^2)\\ &>\frac{1}{1+(\eta-\Delta+1)\kappa}\\ &\quad\times(1-(\eta+\Delta)\kappa-((\eta+\Delta)\kappa)^2)=0\end{aligned}\tag{88}$$

since $1-\tau-\tau^2=0$ and $(\eta+\Delta)\kappa=\tau$. As to the second inequality of (85) we have

$$\begin{aligned}&1-(\eta+\Delta+1+\frac{\eta+\Delta}{1+(\eta+\Delta+1)\kappa})\ln(1+\kappa)\\ &<1-(\eta+\Delta+1+\frac{\eta+\Delta}{1+(\eta+\Delta+1)\kappa})(\kappa-\frac{1}{2}\kappa^2)\\ &=\frac{1}{1+(\eta+\Delta+1)\kappa}\Big(1-(\eta+\Delta)\kappa-((\eta+\Delta)\kappa)^2-\\ &\kappa^2(\eta+\Delta+1/2-\frac{1}{2}(\eta+\Delta+1)^2\kappa)\Big).\end{aligned}\tag{89}$$

As before

$$1-(\eta+\Delta)\kappa-((\eta+\Delta)\kappa)^2=0\tag{90}$$

and

$$\begin{aligned}&\eta+\Delta+\frac{1}{2}-\frac{1}{2}(\eta+\Delta+1)^2\kappa\\ &=\eta+\Delta+\frac{1}{2}-\frac{(\eta+\Delta+1)^2}{2(\eta+\Delta)}\tau.\end{aligned}\tag{91}$$

With $\xi=\eta+\Delta-1$, the right-hand side of (91) becomes

$$\xi+\frac{3}{2}-\frac{(\xi+2)^2}{2(\xi+1)}\tau,\tag{92}$$

and this is positive since $\tau = \frac{1}{2}(\sqrt{5}-1) < \frac{3}{4}$ and $\xi > 0$. This shows the second inequality in (85).

We next prove Theorem 2(ii), and for this we need the following result:

Proposition 9. *With $\beta = \eta + \gamma$ where $-\Delta \le \gamma \le \Delta$,*

$$\sigma(\beta) = \mu(1+\mu)^{\eta+\gamma}, \tag{93}$$

where

$$\begin{aligned} \mu =& \frac{\tau}{\eta+\alpha+\mathcal{O}(\eta^{-1})}, \\ \alpha =& \frac{(2\Delta+3+2\gamma)\tau+2\Delta-1}{2(2\tau+1)}, \end{aligned} \tag{94}$$

and the $\mathcal{O}$ holds uniformly in $\gamma \in [-\Delta, \Delta]$.

Proof: We have $\sigma(\beta) = \mu(1+\mu)^{\beta}$ where μ is the unique solution of the equation

$$(\eta+\Delta+1+\frac{\beta}{1+(1+\beta)\mu})\ln(1+\mu) = 1. \tag{95}$$

We know from the proof of Theorem 2(i) that $\mu = \mathcal{O}(\eta^{-1})$. Multiplying (95) by $1+(1+\beta)\mu$ and expanding

$$\ln(1+\mu) = \mu - \frac{1}{2}\mu^2 + \mathcal{O}(\mu^3), \tag{96}$$

we get

$$\begin{aligned} &(\eta\beta + \frac{1}{2}\eta + (\Delta+\frac{1}{2})\beta + \frac{1}{2}\Delta + \frac{1}{2})\mu^2 + (\eta+\Delta)\mu - 1 \\ &= \frac{1}{2}(\eta+\Delta+1)(\beta+1)\mu^3 + \mathcal{O}(\eta^{-2}). \end{aligned} \tag{97}$$

Next let $\alpha \in \mathbb{R}$ be independent of η and use $\beta = \eta + \gamma$ to write

$$\begin{aligned} &\eta\beta + \frac{1}{2}\eta + (\Delta+\frac{1}{2})\beta + \frac{1}{2}\Delta + \frac{1}{2} = (\eta+\alpha)^2 \\ &+ (\Delta+1+\gamma-2\alpha)\eta + (\Delta+\frac{1}{2})\gamma + \frac{1}{2}\Delta + \frac{1}{2} - \alpha^2. \end{aligned} \tag{98}$$

Together with $\eta+\Delta = \eta+\alpha+\Delta-\alpha$, we obtain

$$\begin{aligned} &(\eta+\alpha)^2\mu^2 + (\eta+\alpha)\mu - 1 = \frac{1}{2}(\eta+\Delta+1)(\eta+\gamma+1)\mu^3 \\ &- (\Delta-\alpha)\mu + \mathcal{O}(\eta^{-2}) - ((\Delta+1+\gamma-2\alpha)\eta \\ &+ (\Delta+\frac{1}{2})\gamma + \frac{1}{2}\Delta + \frac{1}{2} - \alpha^2)\mu^2. \end{aligned} \tag{99}$$

We now take α such that the whole second term in (99) is $\mathcal{O}(\eta^{-2})$. Using that $\mu = \frac{\tau}{\eta} + \mathcal{O}(\eta^{-2})$, this leads to

$$\frac{1}{2}\tau^3 - (\Delta+1+\gamma-2\alpha)\tau^2 - (\Delta-\alpha)\tau = 0, \tag{100}$$

and this yields the α in (94). The polynomial x^2+x-1 has a zero of first order at $x=\tau$. Hence with α as in (94) we see from $(\eta+\alpha)^2\mu^2 + (\eta+\alpha)\mu - 1 = \mathcal{O}(\eta^{-2})$ that $(\eta+\alpha)\mu = \tau + \mathcal{O}(\eta^{-2})$, and this yields $\mu = \tau(\eta+\alpha+O(\eta^{-1})$. ■

Now we proceed to prove Theorem 2(ii). We use the result of Proposition 9. Thus

$$\sigma(\eta+\gamma) = \mu(1+\mu)^{\eta+\gamma}, \tag{101}$$

$$\mu = \frac{\tau}{\eta+\alpha+\mathcal{O}(\eta^{-1})} = \frac{\tau}{\eta+\alpha}(1+\mathcal{O}(\eta^{-2})). \tag{102}$$

By elementary considerations

$$\begin{aligned} &\sigma(\eta+\gamma) \\ &= \frac{\tau}{\eta+\alpha}(1+\frac{\tau}{\eta+\alpha})^{\eta+\gamma}(1+\mathcal{O}(\eta^{-2})) \\ &= \frac{\tau}{\eta+\alpha}\exp[(\eta+\gamma)(\frac{\tau}{\eta+\alpha} - \frac{\tau^2}{2(\eta+\alpha)})](1+\mathcal{O}(\eta^{-2})) \\ &= \frac{\tau e^{\tau}}{\eta+\alpha}(1+\frac{(\gamma-\alpha)\tau - \frac{1}{2}\tau^2}{\eta})(1+\mathcal{O}(\eta^{-2})). \end{aligned} \tag{103}$$

Then letting $\gamma = \pm\Delta$ and

$$\begin{aligned} \alpha(\Delta) &= \frac{(4\Delta+3)\tau+2\Delta-1}{2(2\tau+1)}, \\ \alpha(-\Delta) &= \frac{3\tau+2\Delta-1}{2(2\tau+1)} \end{aligned} \tag{104}$$

in accordance with Proposition 9, it follows that

$$\begin{aligned} &\sigma(\eta+\Delta) - \sigma(\eta-\Delta) = \frac{\tau e^{\tau}}{\eta^2}\Big(\alpha(-\Delta) - \alpha(\Delta) \\ &+ (\Delta-\alpha(\Delta))\tau + (\Delta+\alpha(-\Delta))\tau\Big) + \mathcal{O}(\eta^{-3}) \\ &= \frac{\tau e^{\tau}}{\eta^2}\frac{2\tau^2\Delta}{2\tau+1} + \mathcal{O}(\eta^{-3}). \end{aligned} \tag{105}$$

Finally, it follows easily from $\tau^2+\tau=1$ that $\tau^3(7+4\tau) = 2\tau+1$.

E. Proof of Proposition 5

Since $\sigma > 0$ is fixed, it follows from (see the proof of Theorem 2)

$$\sigma_{\max} < \sigma_+ = \frac{\tau}{\eta+\Delta}\left(1+\frac{\tau}{\eta+\Delta}\right)^{\eta+\Delta} < \frac{\tau e^{\tau}}{\eta+\Delta} \tag{106}$$

that $\sigma_{\max} < \sigma$ when η is large enough. Then by Theorem 1

$$\begin{aligned} \max\theta = \theta(\eta+\Delta) &= \frac{\lambda_0 - 1}{(\eta+\Delta+1)\lambda_0 - \eta - \Delta} \\ &= \frac{\mu_0}{(\eta+\Delta+1)\mu_0 + \Delta} \\ &= \frac{1}{\eta+\Delta+1}\frac{1}{1+\frac{1}{(\eta+\Delta+1)\mu_0}}, \end{aligned} \tag{107}$$

where μ_0 is the unique positive real μ root of $\mu(1+\mu)^{\eta+\Delta} = \sigma$. We shall show that

$$(\eta+\Delta+1)\mu_0 \ge \ln\sigma, \tag{108}$$

$$(\eta+\Delta+1)\mu_0 = \ln(\eta+\Delta) + \mathcal{O}(\ln\ln(\eta+\Delta)), \tag{109}$$

as $\eta \to \infty$, uniformly in $\sigma \in [\epsilon, M]$, where $\epsilon > 0$ and $M > \epsilon$ are fixed. To show (108), we note from $\mu_0(1+\mu_0)^{\eta+\Delta} = \sigma$ that

$$(\eta+\Delta)\mu_0 \ge (\eta+\Delta)\ln(1+\mu_0) = \ln\sigma - \ln\mu_0. \tag{110}$$

Next $\sigma = \mu_0(1+\mu_0)^{\eta+\Delta} \ge \mu_0^{\eta+\Delta+1}$, and so $\ln\mu_0 \le \frac{1}{\eta+\Delta+1}\ln\sigma$. Therefore

$$(\eta+\Delta)\mu_0 \ge \ln\sigma - \frac{1}{\eta+\Delta+1}\ln\sigma = \frac{\eta+\Delta}{\eta+\Delta+1}\ln\sigma, \tag{111}$$

and (108) follows. As to (109), we first observe from (63) that μ_0 decreases in η when $\sigma > 0$ is fixed. Hence $L = \lim_{\eta\to\infty}\mu_0$

exists, and it follows from $\mu_0(1+\mu_0)^{\eta+\Delta}=\sigma$ that $L=0$. Thus, μ_0 decreases to 0 as $\eta\to\infty$. Then, from (110) we get that $(\eta+\Delta)\mu_0$ increases to ∞ as $\eta\to\infty$. All this holds uniformly in $\sigma\in[\epsilon,M]$: Since μ_0 increases in σ, the right-hand side of (110) is bounded below by $\ln\epsilon-\ln\mu_0(\sigma=M)$. Now take $\eta_0>0$ such that $(\eta+\Delta)\mu_0\geq\sigma$ when $\eta\geq\eta_0$ and $\epsilon\leq\sigma\leq M$. Then from $\mu_0(1+\mu_0)^{\eta+\Delta}=\sigma$ we have

$$\begin{aligned}(\eta+\Delta)\ln(1+\mu_0)&=\ln\sigma-\ln\mu_0\\ &\leq\ln(\eta+\Delta)\mu_0-\ln\mu_0\leq\ln(\eta+\Delta)\end{aligned}\tag{112}$$

when $\eta\geq\eta_0$ and $\epsilon\leq\sigma\leq M$. Hence, when $\eta\geq\eta_0$,

$$\begin{aligned}\mu_0&\leq\exp\left[\frac{\ln(\eta+\Delta)}{\eta+\Delta}\right]-1\\ &=\frac{\ln(\eta+\Delta)}{\eta+\Delta}+\mathcal{O}\Big(\Big(\frac{\ln(\eta+\Delta)}{\eta+\Delta}\Big)^2\Big),\end{aligned}\tag{113}$$

where the $\mathcal{O}$ holds uniformly in $\sigma\in[\epsilon,M]$. Then, by (110),

$$\begin{aligned}(\eta+\Delta)\mu_0&\geq\ln\sigma-\ln\left(\exp\left[\frac{\ln(\eta+\Delta)}{\eta+\Delta}\right]-1\right)\\ &=\ln\sigma-\ln(\frac{\ln(\eta+\Delta)}{\eta+\Delta}\left(1+\mathcal{O}\left(\frac{\ln(\eta+\Delta)}{\eta+\Delta}\right)\right)\\ &=\ln(\eta+\Delta)-\ln\ln(\eta+\Delta)\\ &\quad+\ln\sigma+\mathcal{O}\left(\frac{\ln(\eta+\Delta)}{\eta+\Delta}\right),\end{aligned}\tag{114}$$

with $\mathcal{O}$ holding uniformly in $\sigma\in[\epsilon,M]$ and $\eta\geq\eta_0$. From (113) and (114) we get (108) uniformly in $\sigma\in[\epsilon,M]$.

F. *Proof of Theorem 3*

Recall that $\mu_0=\lambda_0-1$. The proof of Theorem 3 requires the following result.

Lemma 1. *If*

$$\Big(\eta+\Delta+1+\frac{\beta}{1+(\beta+1)\mu_0}\Big)\ln(1+\mu_0)=1,\tag{115}$$

then we have that $\mu_0<(\eta+\Delta+1/2)^{-1}$.

Proof: When μ_0 satisfies (115), we have that

$$(\eta+\Delta+1)\ln(1+\mu_0)<1.\tag{116}$$

Now, for $x\geq1$, we have that

$$\begin{aligned}(x+\frac{1}{2})\ln(1+\frac{1}{x})&=x\Big(\frac{1}{x}-\frac{1}{2x^2}+\frac{1}{3x^3}-\frac{1}{4x^4}+\dots\Big)\\ &\quad+\frac{1}{2x}-\frac{1}{4x^2}+\frac{1}{6x^3}-\frac{1}{8x^4}+\dots\\ &=1+\sum_{n=2}^{\infty}(-1)^n(\frac{1}{n+1}-\frac{1}{2n})\frac{1}{x^n}.\end{aligned}\tag{117}$$

We have

$$\Big(\frac{1}{n+1}-\frac{1}{2n}\Big)\Big|_{n=2}=\Big(\frac{1}{n+1}-\frac{1}{2n}\Big)\Big|_{n=3}=\frac{1}{12},\tag{118}$$

and

$$\frac{\mathrm{d}}{\mathrm{d}n}\Big(\frac{1}{n+1}-\frac{1}{2n}\Big)=\frac{(n+1)^2-2n^2}{2n^2(n+1)^2}<0,\quad n\geq3.\tag{119}$$

Hence, when $x\geq1$, the series in (117) is alternating, with terms decreasing monotonically to 0 in modulus and has a positive first term. Hence

$$(x+\frac{1}{2})\ln(1+\frac{1}{x})>1,\quad x\geq1\tag{120}$$

Taking $x=\eta+\Delta+1/2$ in (120), it is seen that

$$(\eta+\Delta+1)\ln\Big(1+\frac{1}{\eta+\Delta+1/2}\Big)>1,\tag{121}$$

and so, from (116), $\mu_0<(\eta+\Delta+\frac{1}{2})^{-1}$, as required. ■

We now proceed to prove Theorem 3. We want to show that $\theta(\sigma,\beta^*(\sigma))$ is increasing in $\sigma>0$. For $\sigma\geq\sigma_{\max}$ we have by Theorem 1 that $\beta^*(\sigma)=\eta+\Delta$, and it readily follows from Corollary 1 and (74) that $\theta(\sigma,\beta^*(\sigma))$ is increasing in $\sigma\geq\sigma_{\max}$.

Let $\sigma\leq\sigma_{\max}$, and observe that

$$\begin{aligned}\frac{\mathrm{d}}{\mathrm{d}\sigma}[\theta(\beta^*(\sigma),\sigma)]&=\frac{\partial\theta}{\partial\beta}(\beta^*(\sigma),\sigma)\frac{\mathrm{d}\beta^*}{\mathrm{d}\sigma}(\sigma)\\ &+\frac{\partial\theta}{\partial\sigma}(\beta^*(\sigma),\sigma)=\frac{\partial\theta}{\partial\sigma}(\beta^*(\sigma),\sigma).\end{aligned}\tag{122}$$

Here it has been used that

$$\begin{aligned}&\frac{\mathrm{d}\beta^*}{\mathrm{d}\sigma}(\sigma)=0,\ \sigma\notin[\sigma_{\min},\sigma_{\max}];\\ &\frac{\partial\theta}{\partial\beta}(\beta^*(\sigma),\sigma)=0,\ \sigma\in[\sigma_{\min},\sigma_{\max}].\end{aligned}\tag{123}$$

Let $\eta-\Delta\leq\beta\leq\eta+\Delta$ and set $\delta=\eta+\Delta-\beta\in[0,2\Delta]$. Rewriting (17), we have

$$\theta(\beta,\sigma)=\frac{(\lambda_0-1)\lambda_0^{-\delta}}{(\beta+1)\lambda_0-\beta}=\frac{\mu_0(1+\mu_0)^{-\delta}}{\beta\mu_0+\mu_0+1},\tag{124}$$

and we compute

$$\begin{aligned}\frac{\partial\theta}{\partial\sigma}(\beta,\sigma)&=\frac{\partial}{\partial\sigma}\Big(\frac{\mu_0(1+\mu_0)^{-\delta}}{\beta\mu_0+\mu_0+1}\Big)\\ &=\frac{\mathrm{d}}{\mathrm{d}\mu}\Big(\frac{\mu(1+\mu)^{-\delta}}{\beta\mu+\mu+1}\Big)\Big|_{\mu=\mu_0}\frac{\partial\mu_0}{\partial\sigma}(\beta,\sigma).\end{aligned}\tag{125}$$

Since by (74), $\frac{\partial\mu_0}{\partial\sigma}(\beta,\sigma)>0$, we have that

$$\frac{\partial\theta}{\partial\sigma}(\beta,\sigma)>0\Leftrightarrow\frac{\mathrm{d}}{\mathrm{d}\mu}\Big(\frac{\mu(1+\mu)^{-\delta}}{\beta\mu+\mu+1}\Big)\Big|_{\mu=\mu_0}>0.\tag{126}$$

We compute

$$\begin{aligned}&\frac{\mathrm{d}}{\mathrm{d}\mu}\Big(\frac{\mu(1+\mu)^{-\delta}}{\beta\mu+\mu+1}\Big)\\ &=\frac{(1+\mu)^{-\delta-1}}{(\beta\mu+\mu+1)^2}\big(1+(1-\delta)\mu-\delta(1+\beta)\mu^2\big),\end{aligned}\tag{127}$$

so (126) can be rewritten as

$$\frac{\partial\theta}{\partial\sigma}(\beta,\sigma)>0\Leftrightarrow\delta(1+\beta)\mu^2+(\delta-1)\mu\Big|_{\mu=\mu_0}<1.\tag{128}$$

Thus we have to verify the second member of (128) for the special case that $\beta=\beta^*(\sigma)$. When $\sigma\leq\sigma_{\min}$, we have $\beta^*(\sigma)=\eta-\Delta$, $\delta=2\Delta$, and the second member of (128) turns into

$$2\Delta\eta\mu_0^2+(2\Delta-1)\mu_0<1.\tag{129}$$

Now μ_0 increases in $\sigma \in [0, \sigma_{\min}]$, and so $2\Delta\eta\mu_0^2+(2\Delta-1)\mu_0$ is maximal when $\sigma = \sigma_{\min}$. Hence, it suffices to check the second member of (128) for the case that $\sigma \in [\sigma_{\min}, \sigma_{\max}]$.

When $\delta \leq 1$, we have from $\mu_0 < (\eta + \Delta + 1/2)^{-1}$ that

$$\delta(1+\beta)\mu_0^2 + (\delta-1)\mu_0 \leq \frac{1+\beta}{(\eta+\Delta+1/2)^2} \leq \frac{\eta+\Delta+1}{(\eta+\Delta+1/2)^2} < 1. \tag{130}$$

When $\delta > 1$, the function $\mu > 0 \mapsto \delta(1+\beta)\mu^2 + (\delta-1)\mu$ is increasing, and so, from Lemma 1, using $\beta = \eta + \Delta - \delta$, we get

$$\delta(1+\beta)\mu_0^2 + (\delta-1)\mu_0 < (\delta-1)\frac{1}{\eta+\Delta+\frac{1}{2}} + \delta(\eta+\Delta+1-\delta)\Big(\frac{1}{\eta+\Delta+\frac{1}{2}}\Big)^2. \tag{131}$$

Set $\eta + \Delta + 1/2 = A$. We have to check whether

$$\delta(A+\frac{1}{2}-\delta) + (\delta-1)A < A^2. \tag{132}$$

The left-hand side of (132) equals

$$\begin{aligned} & -\delta^2 + 2\big(A+\frac{1}{4}\big)\delta - A \\ =& -\big(\delta - \big(A+\frac{1}{4}\big)\big)^2 - A + \big(A+\frac{1}{4}\big)^2 \\ =& A^2 - \frac{1}{2}A + \frac{1}{16} - \big(\delta - \big(A+\frac{1}{4}\big)\big)^2, \end{aligned} \tag{133}$$

and this is less than A^2 since $A \geq 1/2 > 1/8$.

References

[1] N. Abramson, “The ALOHA system - another alternative for computer communications,” in *Proc. AFIPS*, 1970, pp. 281–285.

[2] S. Asmussen, *Applied Probability and Queues*, 2nd ed. New York: Springer-Verlag, 2003.

[3] Y. Baryshnikov, E. Coffman, Jr., and P. Jelenković, “Space filling and depletion,” *J. Appl. Probab.*, vol. 41, no. 3, pp. 691–702, 2004.

[4] T. Bonald and M. Feuillet, “On the stability of flow-aware CSMA,” *Performance Evaluation*, vol. 67, no. 11, pp. 1219–1229, 2010.

[5] R. Boorstyn and A. Kershenbaum, “Throughput analysis of multihop packet radio,” in *Proc. ICC*, 1980, pp. 1361–1366.

[6] C. Bordenave, D. McDonald, and A. Proutière, “Performance of random medium access control, an asymptotic approach,” in *Proc. ACM SIGMETRICS*, Annapolis, MD, June 2–6 2008, pp. 1–12.

[7] N. de Bruijn, *Asymptotic methods in analysis*, 3rd ed. New York: Dover Publications Inc., 1981.

[8] D. Denteneer, S. Borst, P. van de Ven, and G. Hiertz, “IEEE 802.11s and the philosophers’ problem,” *Statistica Neerlandica*, vol. 62, no. 3, pp. 283–298, 2008.

[9] M. Durvy, O. Dousse, and P. Thiran, “Modeling the 802.11 protocol under different capture and sensing capabilities,” in *Proc. Infocom*, Anchorage, AK, May 6–12 2007, pp. 2356–2360.

[10] ——, “Self-organization properties of CSMA/CA systems and their consequences on fairness,” *IEEE Trans. Inf. Theory*, vol. 55, no. 3, pp. 931–943, 2009.

[11] X. Guo, S. Roy, and W. Conner, “Spatial reuse in wireless ad-hoc networks,” in *Proc. VTC*, 2003, pp. 1437–1442.

[12] Z. Haas and J. Deng, “Dual busy tone multiple access (DBTMA)–a multiple access control scheme for ad hoc networks communication,” *IEEE Trans. Comm.*, vol. 50, no. 6, pp. 975–985, 2002.

[13] L. Jiang and S. Liew, “Improving throughput and fairness by reducing exposed and hidden nodes in 802.11 networks,” *IEEE Trans. Mob. Comp*, vol. 7, no. 1, pp. 34–49, 2008.

[14] L. Jiang and J. Walrand, “A distributed CSMA algorithm for throughput and utility maximization in wireless networks,” in *Proc. 46th Annual Allerton Conf. Commun., Control and Comp.*, 2008, pp. 1511–1519.

[15] F. Kelly, “Loss networks,” *Ann. Appl. Probab.*, vol. 1, no. 3, pp. 319–378, 1991.

[16] L. Kleinrock and F. Tobagi, “Packet switching in radio channels: part I - carrier sense multiple-access modes and their throughput-delay characteristics,” *IEEE Trans. Commun.*, vol. 23, no. 12, pp. 1400–1416, 1975.

[17] T.-Y. Lin and J. Hou, “Interplay of spatial reuse and SINR-determined data rates in CSMA/CA-based, multi-hop, multi-rate wireless networks.” in *Proc. Infocom*, Anchorage, AK, May 6–12 2007, pp. 803–811.

[18] H. Ma, R. Vijaykumar, S. Roy, and J. Zhu, “Optimizing 802.11 wireless mesh networks based on physical carrier sensing,” *IEEE/ACM Trans. Netw.*, vol. 17, no. 5, pp. 1550–1563, 2009.

[19] J. Monks, V. Bharghavan, and W.-M. Hwu, “A power controlled multiple access protocol for wireless packet networks,” in *Proc. Infocom*, Anchorage, AK, May 6–12 2007, pp. 219–228.

[20] A. Muqattash and M. Krunz, “Power controlled dual channel (PCDC) medium access protocol for wireless ad hoc networks,” in *Proc. Infocom*, San Francisco, CA, March 30–April 3 2003, pp. 470–480.

[21] J. Ni, B. Tan, and R. Srikant, “Q-CSMA: queue-length based CSMA/CA algorithms for achieving maximum throughput and low delay in wireless networks,” in *Proc. Infocom*, San Diego, CA, March 15–19 2010.

[22] E. Pinsky and Y. Yemini, “The asymptotic analysis of some packet radio networks,” *IEEE J. Sel. Areas Commun.*, vol. 4, no. 6, pp. 938–945, 1986.

[23] S. Rajagopalan, D. Shah, and J. Shin, “Network adiabatic theorem: an efficient randomized protocol for content resolution,” in *Proc. ACM SIGMETRICS/Performance*, Seattle, WA, June 15–19 2009, pp. 133–144.

[24] P. van de Ven, A. Janssen, and J. van Leeuwaarden, “Optimal tradeoff between exposed and hidden nodes in large wireless networks,” in *Proc. ACM SIGMETRICS*, New York, NY, June 14–18 2010, pp. 179–190.

[25] P. van de Ven, J. van Leeuwaarden, D. Denteneer, and A. Janssen, “Spatial fairness in linear random-access networks,” *Performance Evaluation*, vol. 69, no. 3–4, pp. 121–134, 2012.

[26] X. Wang and K. Kar, “Throughput modelling and fairness issues in CSMA/CA based ad-hoc networks,” in *Proc. Infocom*, Miami, FL, March 13–17 2005, pp. 23–34.

[27] X. Yang and N. Vaidya, “On physical carrier sensing in wireless ad hoc networks,” in *Proc. Infocom*, Miami, FL, March 13–17 2005, pp. 2525–2535.

[28] M. Zafer and E. Modiano, “Blocking probability and channel assignment in wireless networks,” *IEEE Trans. Wireless Commun.*, vol. 5, no. 4, pp. 869–879, 2006.

[29] H. Zhai and Y. Fang, “Physical carrier sensing and spatial reuse in multirate and multihop wireless ad hoc networks,” in *Proc. Infocom*, Barcelona, Spain, April 23–29 2006.

[30] J. Zhu, X. Guo, L. Yang, and W. Conner, “Leveraging spatial reuse in 802.11 mesh networks with enhanced physical carrier sensing,” in *Proc. ICC*, 2004, pp. 4004–4011.